UNIVERSITÀ DI CAMERINO

Chemistry Interdisciplinary Project

NANOSCIENCE AS AN OPPORTUNITY FOR ENVIRONMENTAL APPLICATIONS

Dr. Marco Zannotti

School of Science and Technology, Chemistry Interdisciplinary Project (ChIP), University of Camerino

GRUPPO DI RICERCA CHIMICA ANALITICA AMBIENTALE

Prof.ssa Rita Giovannetti - Prof. Stefano Ferraro

NANOSCIENCE FOR ENVIRONMENT APPLICATIONS

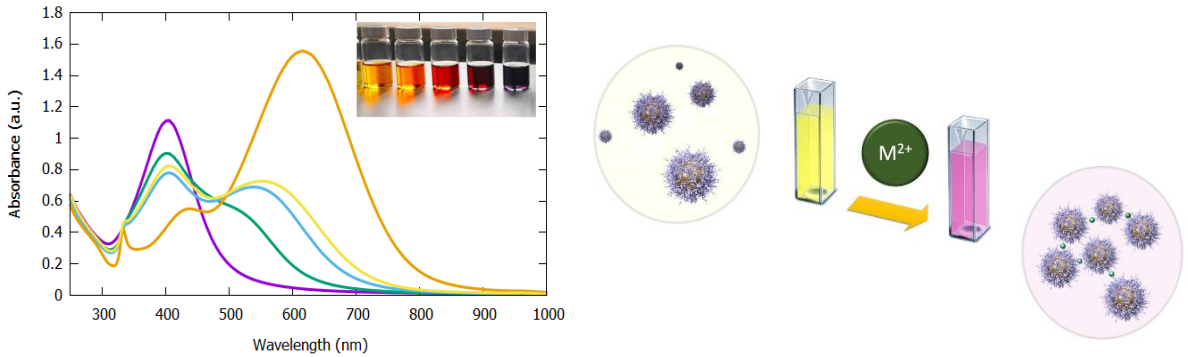

Metal nanoparticles as colorimetric sensors for pollutants detection

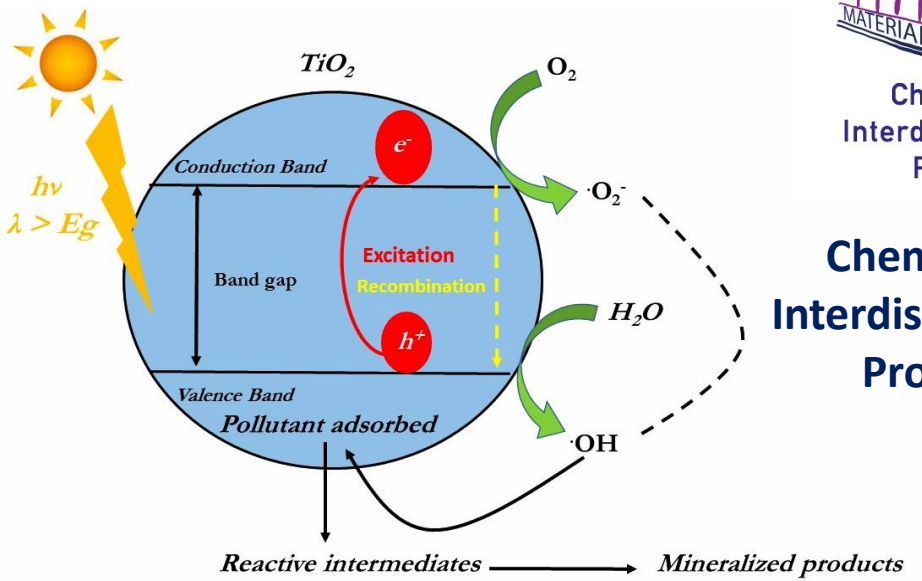

TiO_2-based photocatalysis for environmental remediation

Adsorbent material for environmental application

Chemistry Interdisciplinary Project

Chemistry Interdisciplinary Project

NANOPARTICLES AS SENSOR

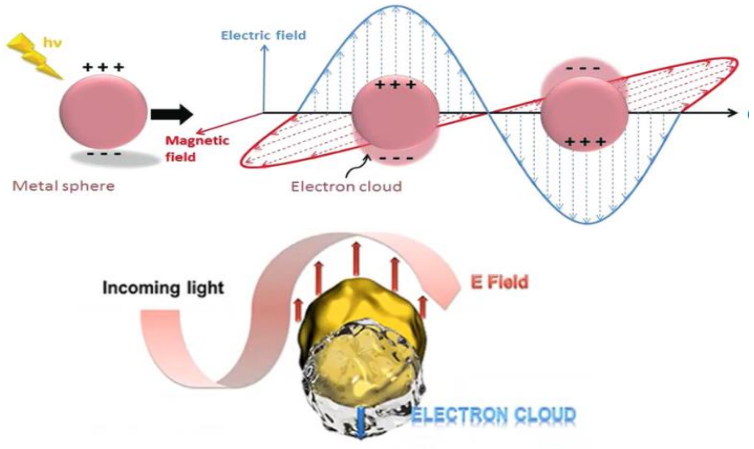

Surface conduction electrons of the metal oscillate coherently with the incident electric field. The applied field induces a polarization of the electrons and a separation of negative and positive charges on the surface of the nanoparticles forming dipoles oscillating along the direction of the electric field.

This behavior is called as ***Surface Plasmon Resonance*** (SPR).

In the case of **Metal Nanoparticles strong absorption in the Visible region.**

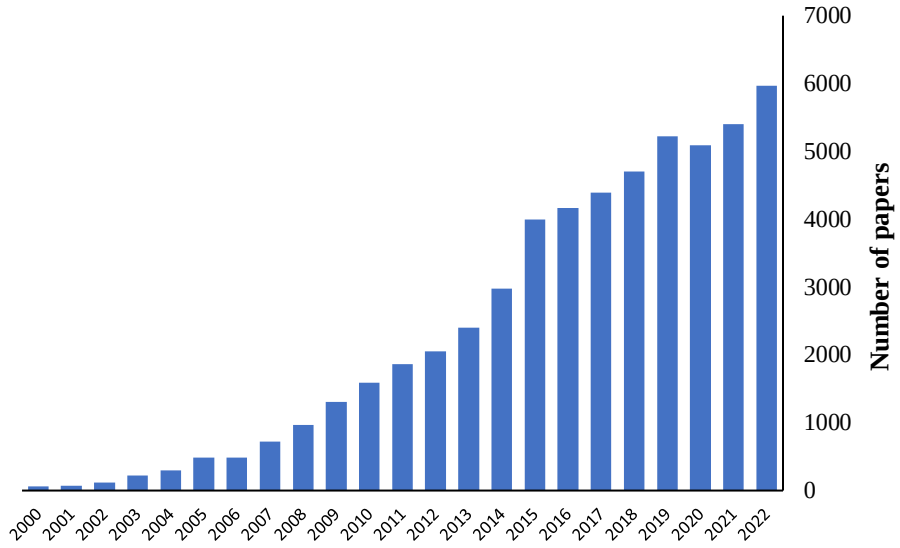

SCOPUS database: keywords "nanoparticle" AND " sensor"

USEFUL INFORMATION:

DIMENSIONS

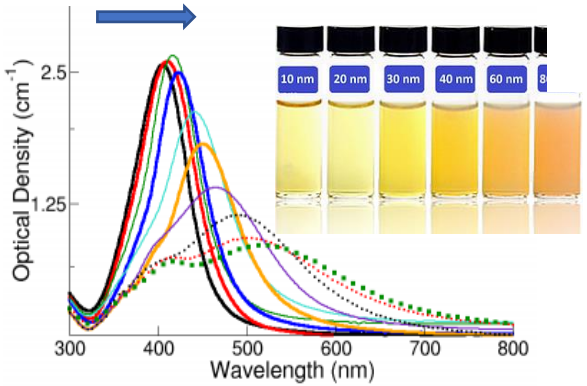

SHAPE

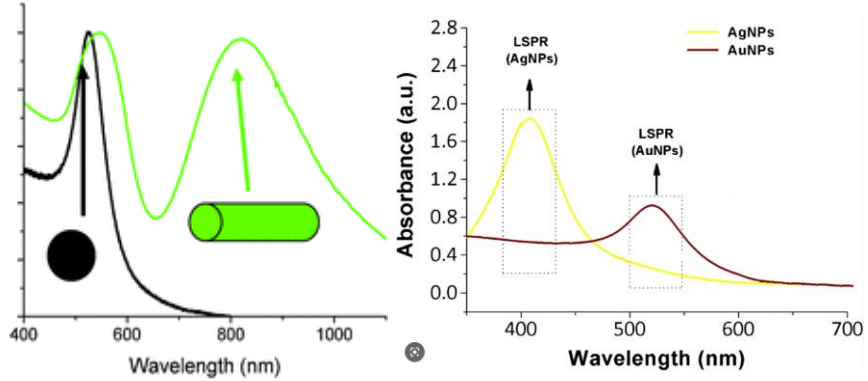

LSPR extreme sensitive to the surrounding environment: COLORIMETRIC SENSOR.

NANOPARTICLES AS SENSOR

Chemistry Interdisciplinary Project

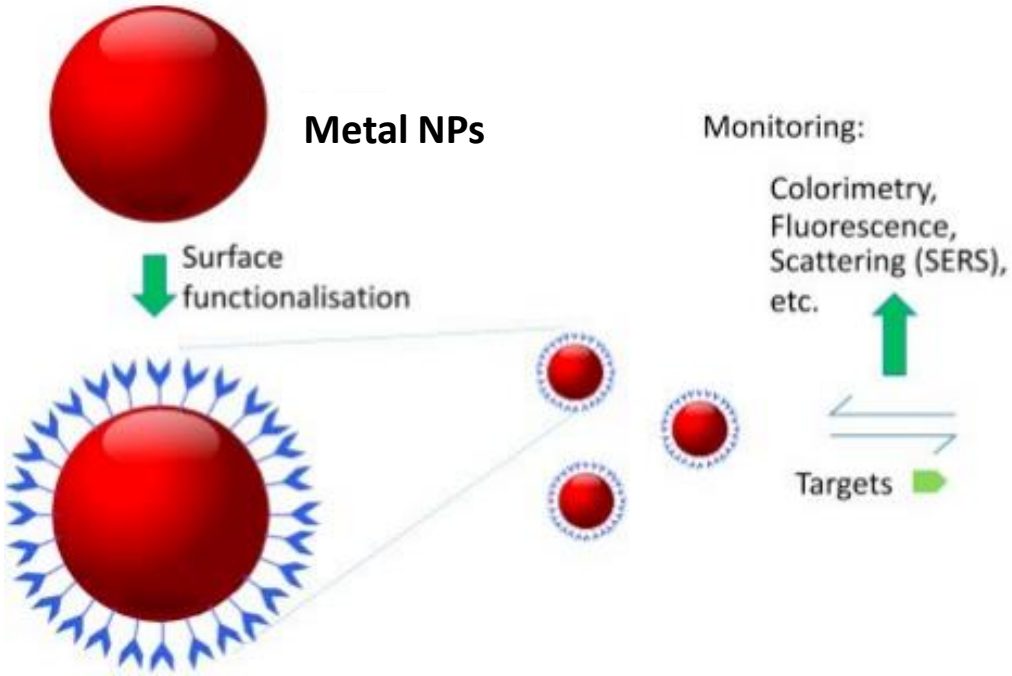

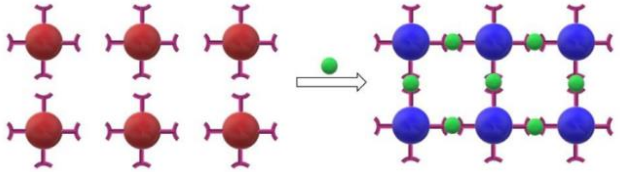

Aggregation Induced by Interparticle Cross-Linking.

or

Binding with specific analyte.

or

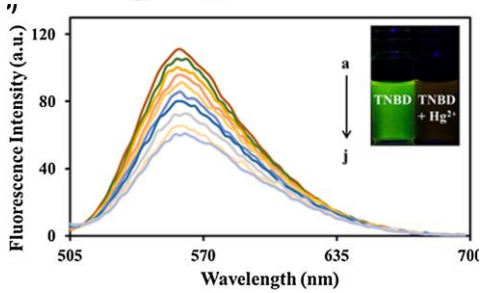

Fluorescence quenching

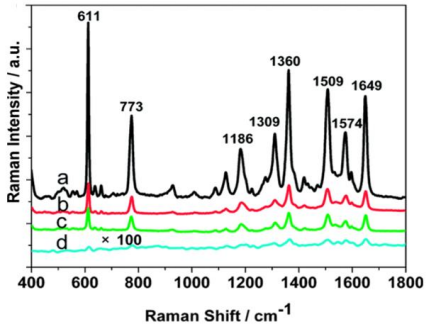

Metal nanoparticles used as SERS activator for Raman Spectroscopy

SINTESI ARCOBALENO: NANOPARTICELLE DI ARGENTO

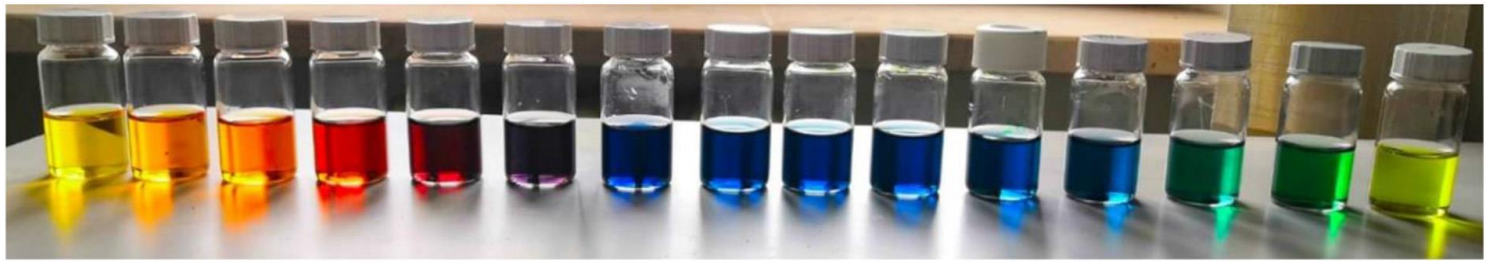

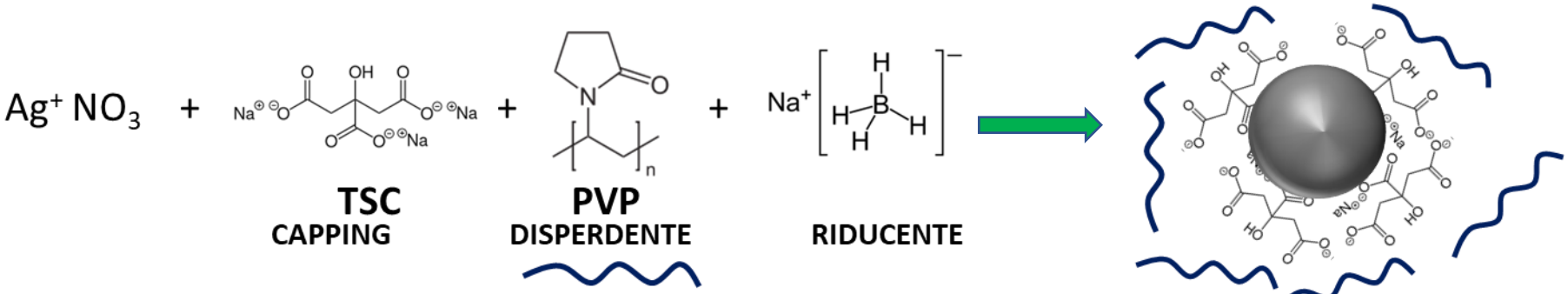

During the synthesis different amounts of H_2O_2 30% have been added.

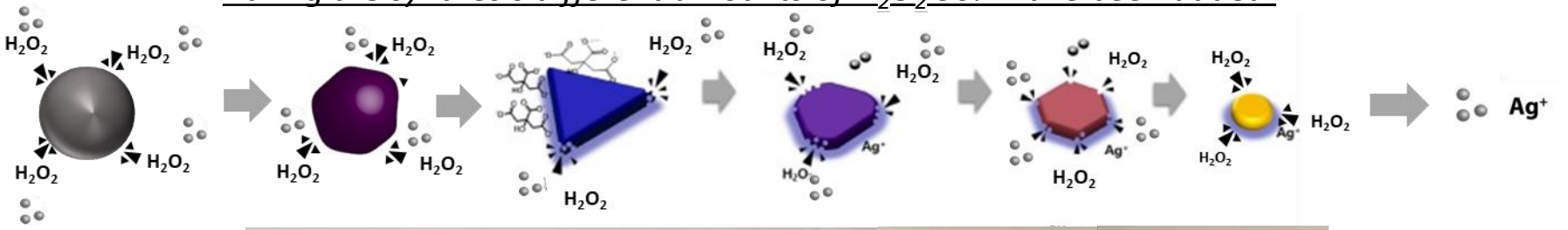

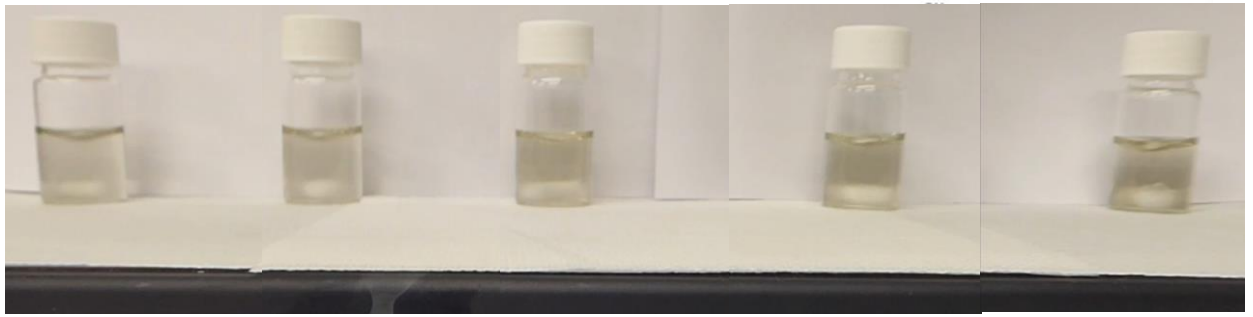

H_2O_2 oxidation etching of Silver Nanoparticles (AgNPs)

Chemistry Interdisciplinary Project

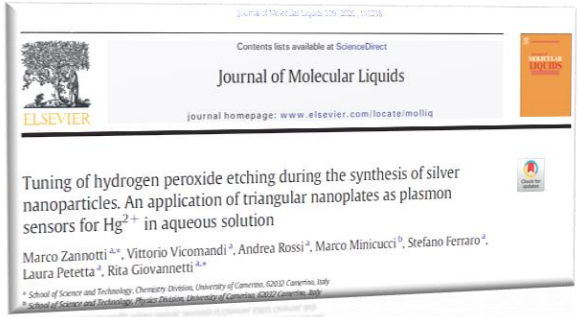
Contents lists available at ScienceDirect

Journal of Molecular Liquids

journal homepage: www.elsevier.com/locate/molliq

Tuning of hydrogen peroxide etching during the synthesis of silver nanoparticles. An application of triangular nanoplates as plasmon sensors for Hg^{2+} in aqueous solution

Marco Zannotti, Vittorio Vicomandi, Andrea Rossi, Marco Minicucci, Stefano Ferraro, Laura Petetta, Rita Giovannetti

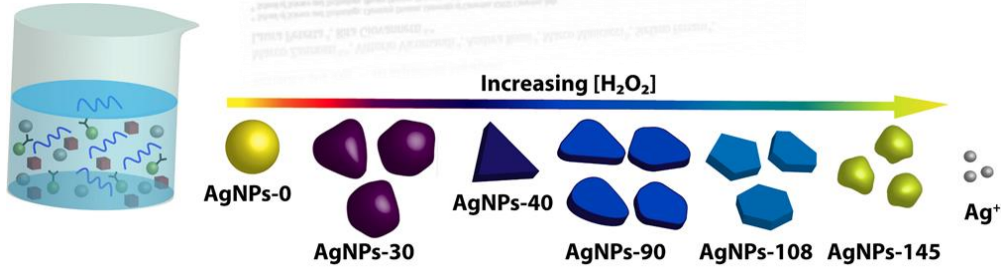

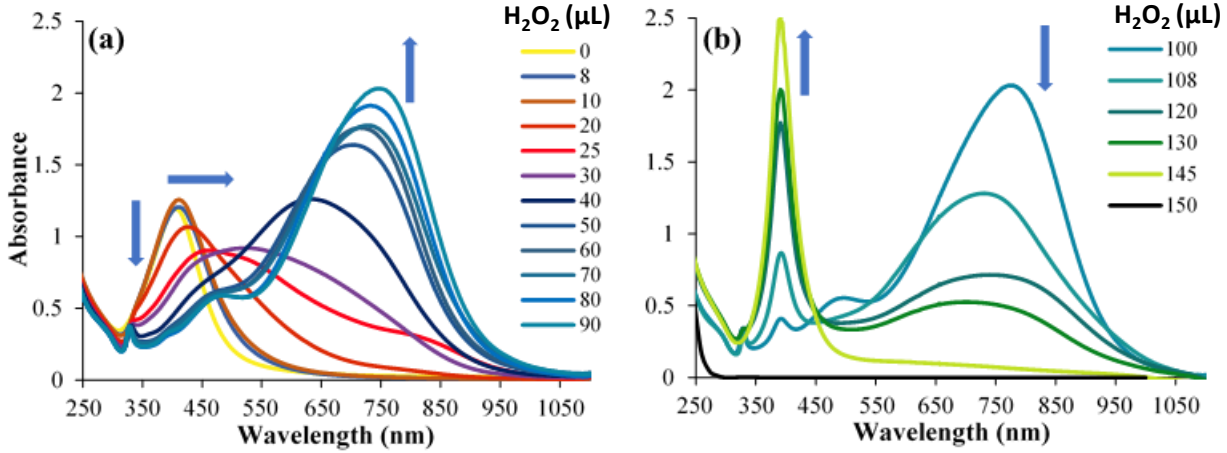

These conditions in presence of TSC and PVP, are ideal for the formation of nanoplates with different shapes in the range between 40 and 108 µl of hydrogen peroxide.

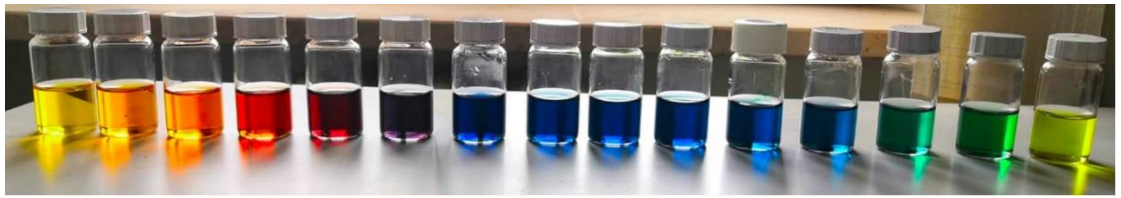

- H_2O_2 shows oxidizing power, standard redox potential depends on the pH, both higher with respect to the standards redox potential of Ag^+;
- pH of AgNPs-0 is at 7.6, in presence of H_2O_2 the range of pH is between 7.5 to 7.8;

$$H_2O_2 + 2Ag \rightleftharpoons 2Ag^+ + 2H_2O \qquad \Delta E^0 = +0.974\ V \text{ acidic solution}$$

$$H_2O_2 + 2Ag \rightleftharpoons 2Ag^+ + OH^- \qquad \Delta E^0 = +0.07\ V \text{ basic solution}$$

- Weak reducing character of H_2O_2, smaller contribution to reducing Ag^+, controlling the shape during the formation of AgNPs;

$$H_2O_2 + 2\,Ag^+ \rightleftharpoons O_2 + 2H^+ + 2\,Ag \qquad \Delta E^0 = +0.104\ V \text{ acidic solution}$$

$$H_2O_2 + 2\,Ag^+ + 2\,OH^- \rightleftharpoons O_2 + 2H_2O + 2\,Ag \qquad \Delta E^0 = +0.946\ V \text{ basic solution}$$

- Dynamic equilibrium between the reduction of Ag^+ by $NaBH_4$ and oxidation of AgNPs by H_2O_2, the weak reducing character of H_2O_2 can also contribute to the shape-controls of AgNPs.

SEM characterization of Silver Nanoparticles (AgNPs)

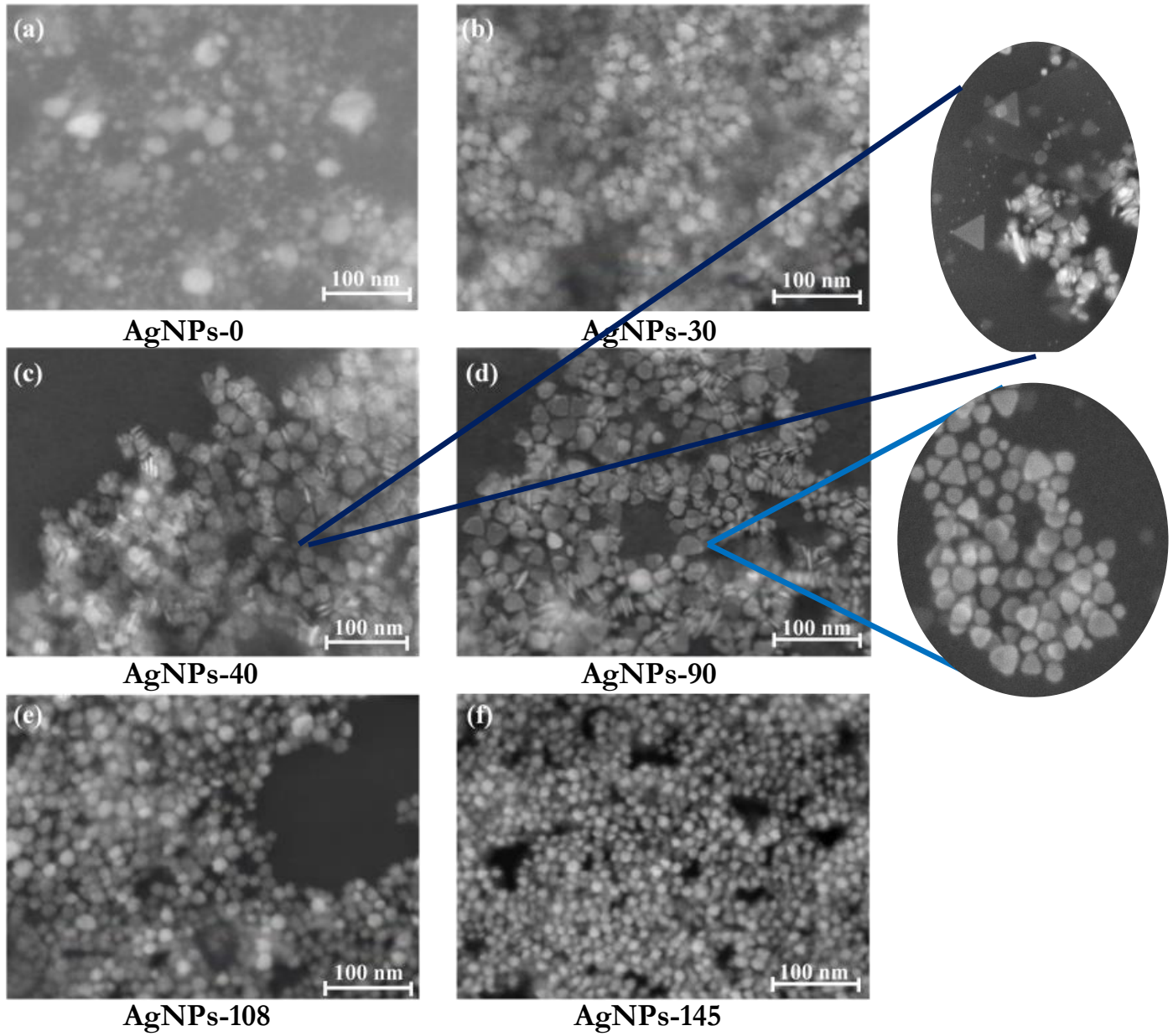

- AgNPs-0: spherical shapes with aggregates, diameter=11 nm;
- AgNPs-30: regular distribution, not well defined shapes, size from 11 to 25 nm;
- AgNPs-40: regular triangular nanoplates, thickness ≈ 5 nm, size= 27-30 nm;
- AgNPs-90: smoothed triangular nanoplates, tendency to form hexagoanl and pentagonal shapes with different sizes and thicknesses;
- AgNPs-108: distribution of hexagonal and pentagonal shapes, size at around 23 nm;
- AgNPs-145: quasi-spherical shapes with samller diameters of 8-10 nm.

Silver Nanoparticles (AgNPs) as sensor for Hg^{2+} ions

Detection of Mercury-LSPR-based colorimetric sensor

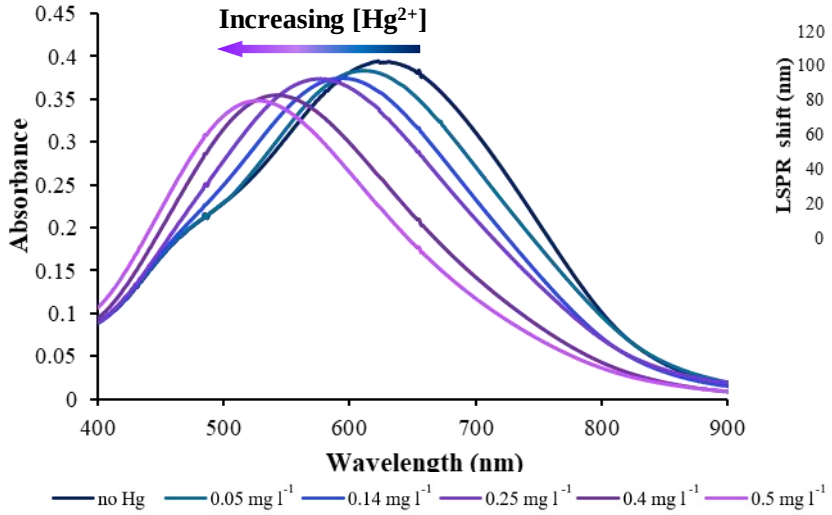

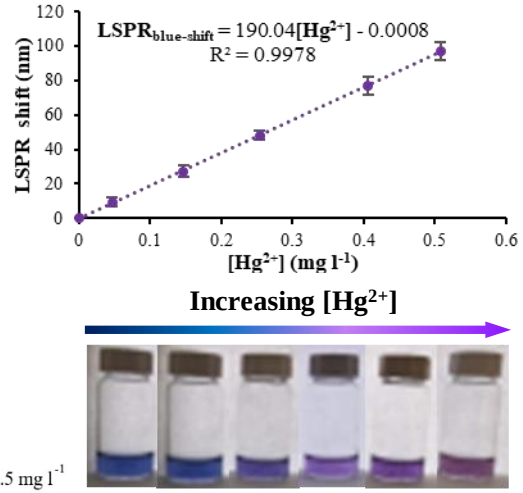

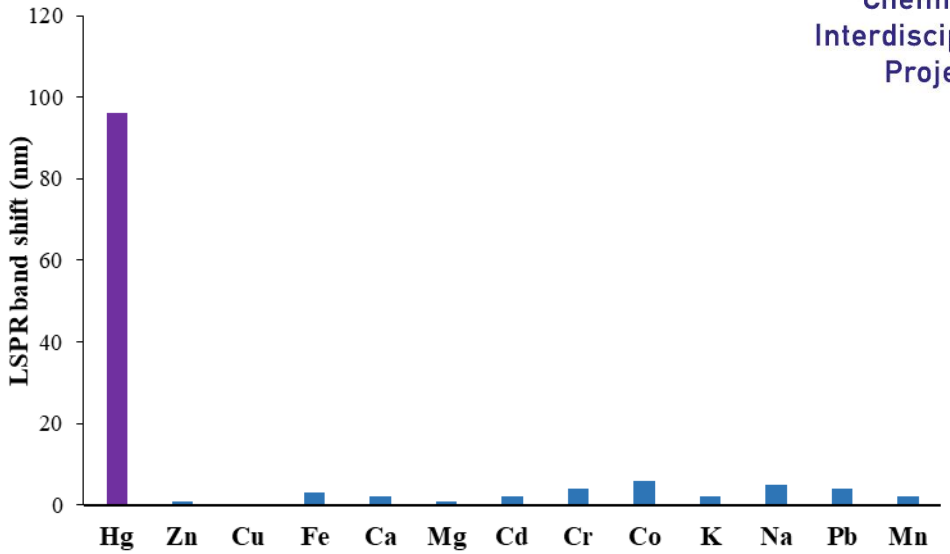

- **AgNPs-40 shows good sensitivity and selectivity towards Hg^{2+} ions**;
- LSPR regular blue-shift with higher concentration of Hg^{2+} ions, from 623 to 527 nm;
- **Linear relation between LSPR shift and concentration of Hg^{2+} ions**;
- LOD, calculated as 3σ/slope is equal to 0.013 mg L^{-1}(64.9 nM).
- SEM analysis show shape modification from triangular nanoplates to hexagons and pentagons shapes

M. Zannotti et al., Journal of Molecular Liquids, 309 (2020) 113238

Silver Nanoparticles (AgNPs) as sensor for Hg^{2+} ions

Detection of Mercury-LSPR-based colorimetric sensor

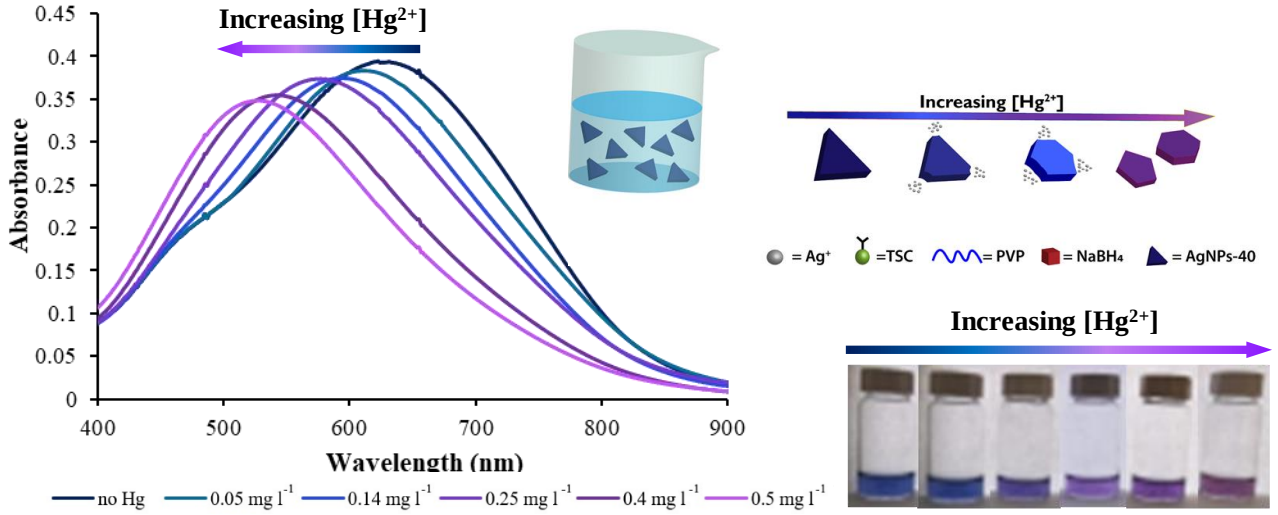

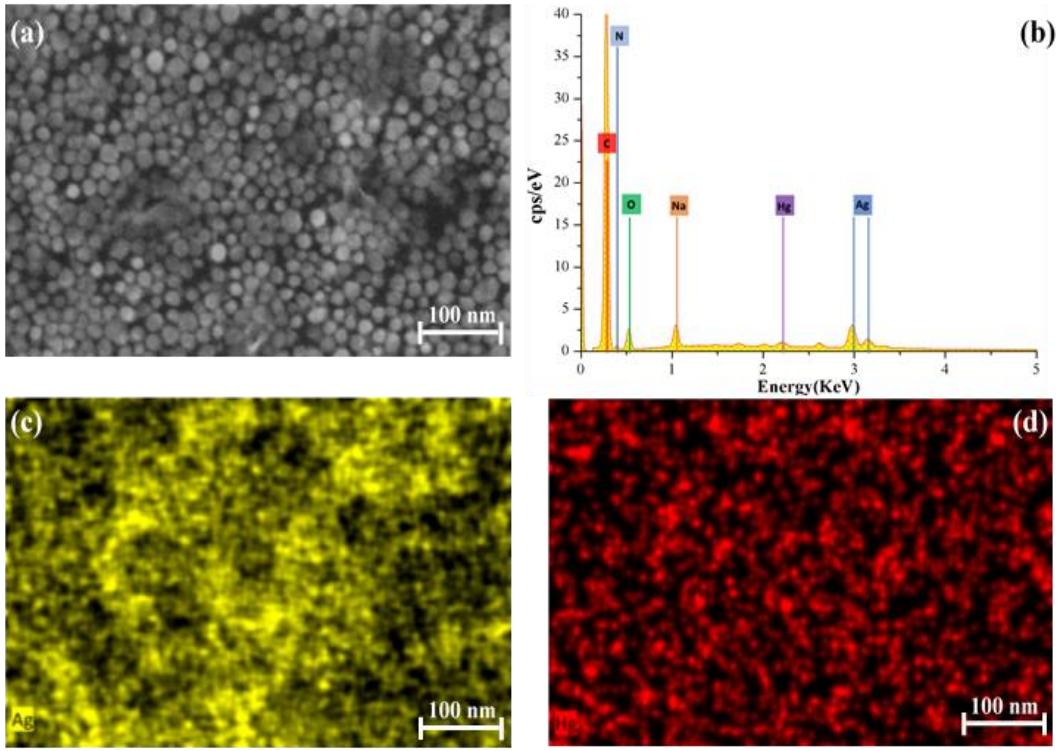

- **AgNPs-40 shows good sensitivity and selectivity towards Hg^{2+} ions**;
- LSPR regular blue-shift with higher concentration of Hg^{2+} ions, from 623 to 527 nm;
- **Linear relation between LSPR shift and concentration of Hg^{2+} ions**;
- LOD, calculated as 3/slope is equal to 0.013 mg L^{-1}(64,9 nM).
- SEM analysis show shape modification from triangular nanoplates to hexagons and pentagons shapes

$$Ag^+ + e^- \rightleftharpoons Ag \qquad E^0 = +0.7996\ V$$

$$Hg^{2+} + 2e^- \rightleftharpoons Hg \qquad E^0 = +0.851\ V$$

$$Hg^{2+} + Ag \rightleftharpoons Hg + Ag^+ \qquad \Delta E^0 = +0.0514\ V$$

M. Zannotti et al., Journal of Molecular Liquids, 309 (2020) 113238

Silver Nanoparticles (AgNPs) as SERS substrate for pollutant detection

AgNPs deposition

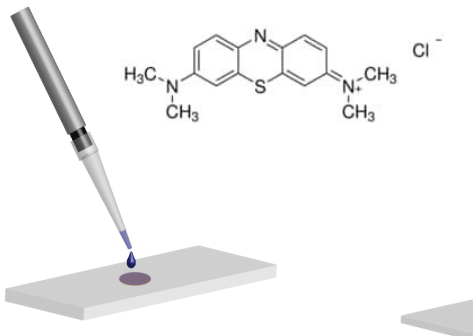

MB deposition

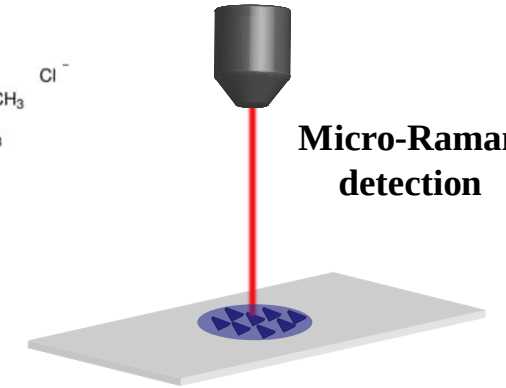

Micro-Raman detection

$$EF = \frac{I_{SERS}/c_{SERS}}{I_{RS}/c_{RS}}$$

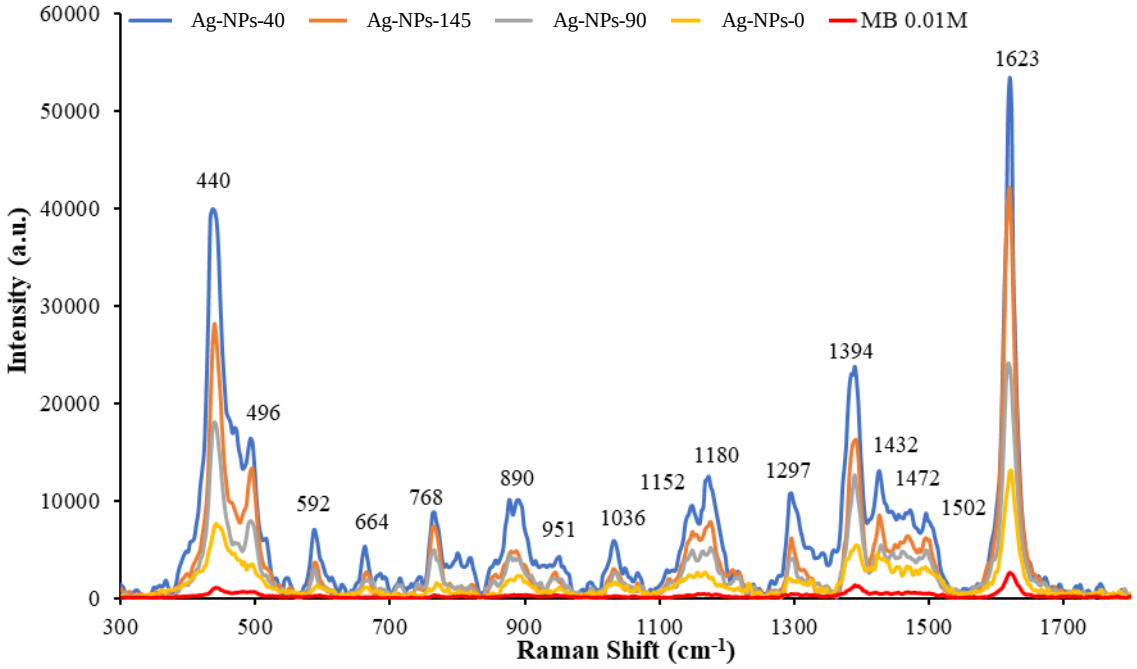

Raman and SERS intensity of MB 1 μM and the calculated AEFs at 440 and 1623 cm^{-1}

Normal Raman	I_{1623}	I_{440}		
MB 0.01 M	2635.57	1085.33		
SERS substrate (MB 1μM)	I_{1623}	**AEF (×10^5)**	I_{440}	**AEF (×10^5)**
AgNPs-0	13126	0.50	7654.16	0.71
AgNPs-90	24130.5	0.92	18111.8	1.67
AgNPs-145	40742.7	**1.55**	28186.4	2.60
AgNPs-40	53480.1	**2.03**	39952.3	3.68

AgNPs-40 > AgNPs-145 > AgNPs-90 > AgNPs-0

M. Zannotti et al., Coatings 2020, 10, 288

Silver Nanoparticles (AgNPs@MUA) –based sensor for the detection of Nickel Ions

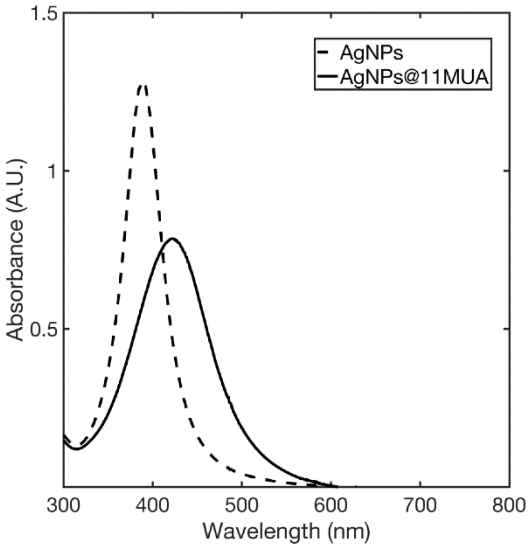

- **AgNPs** sinthesyzed with **$NaBH_4$** as reducing agent were successively functionalized with mercaptoundecanoic acid(**11MUA**);
- **AgNPs@11MUA** were tested as sensor for different heavy metals: Ni, Zn, Cu, Co, Cd,Mn,Hg,Cr,Pb;
- In the range between 0-10uM, only Nickel shows strong interaction with **AgNPs@11MUA** as demonstrated by the typical UV-Vis spectra of AgNPs

Ni^{2+}: strong aggregation

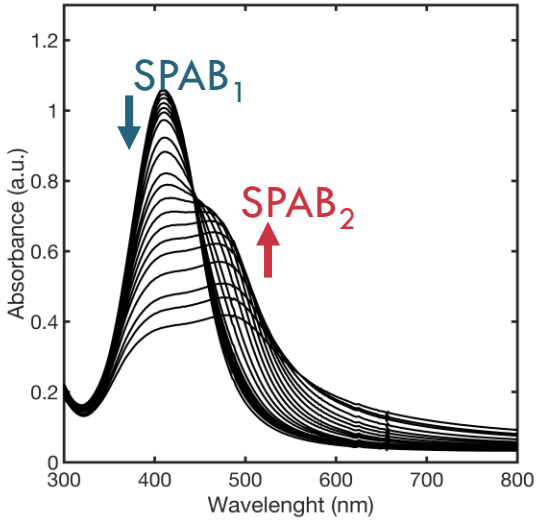

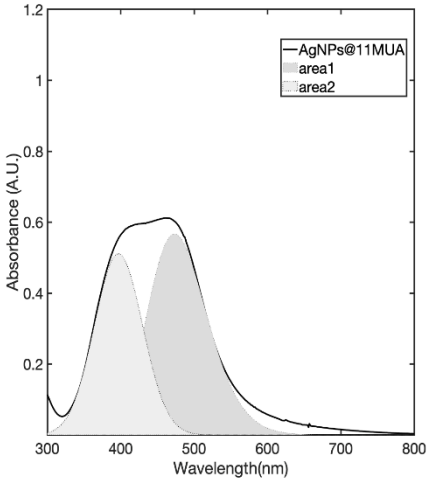

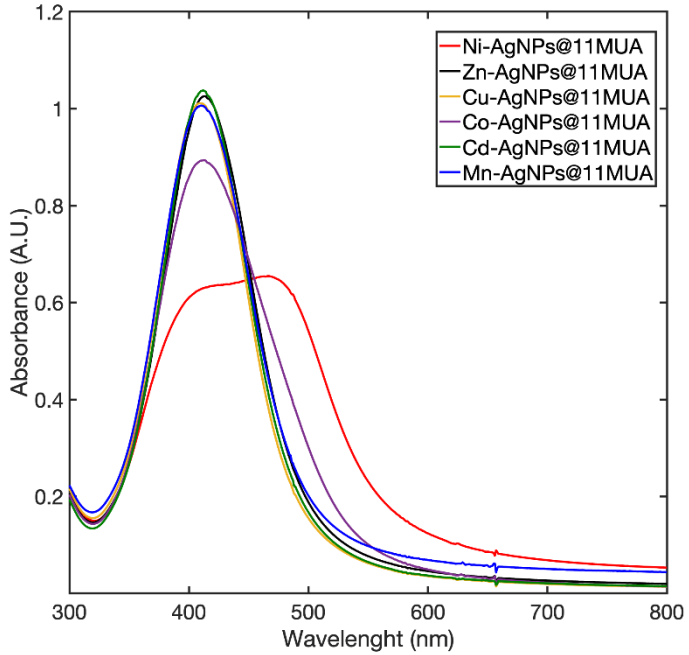

Second Surface Plasmon Resonace band appears, due to the interaction of AgNpS@11MUA and Ni^{2+} ions with concomitant aggregations of nanoparticles

Silver Nanoparticles (AgNPs@MUA) –based sensor for the detection of Nickel Ions

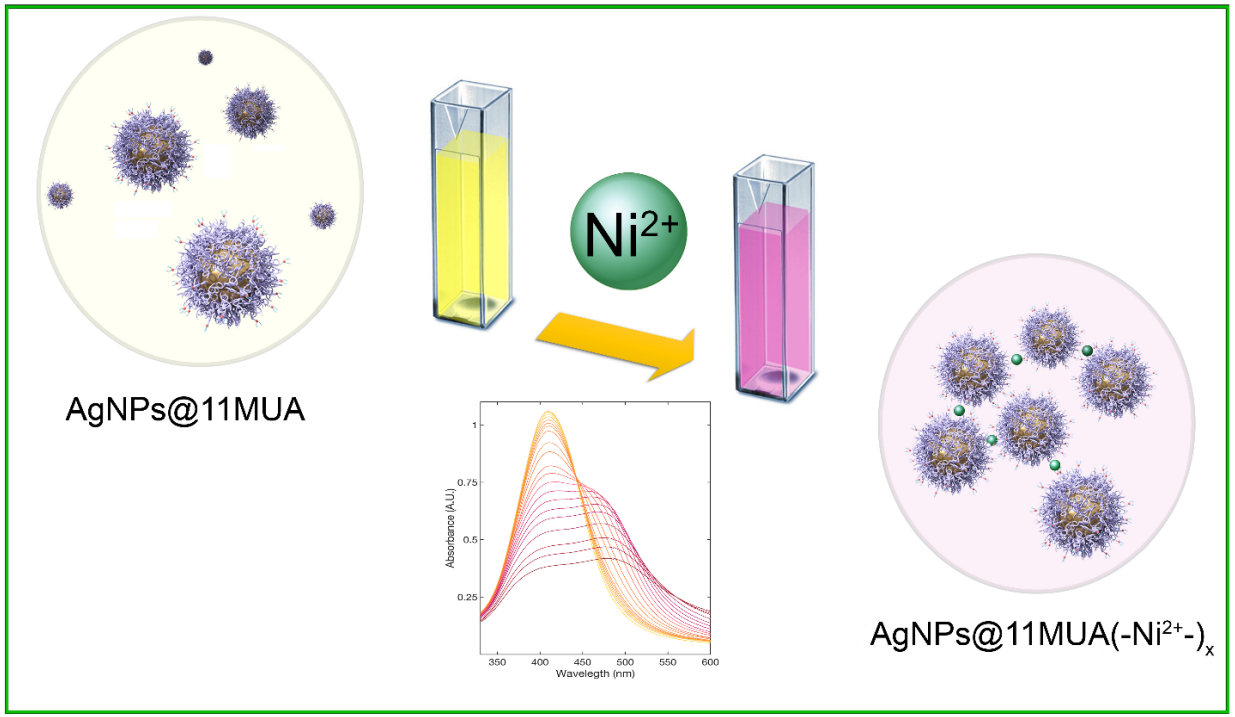

Second Surface Plasmon Resonace band appears, due to the interaction of AgNpS@11MUA and Ni^{2+} ions with concomitant aggregations of nanoparticles

Silver Nanoparticles (AgNPs@MUA) –based sensor for the detection of Nickel Ions

Titration curve can be divided in three different regions

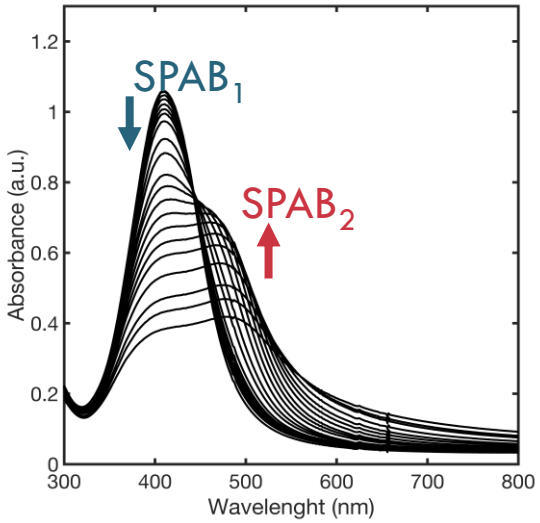

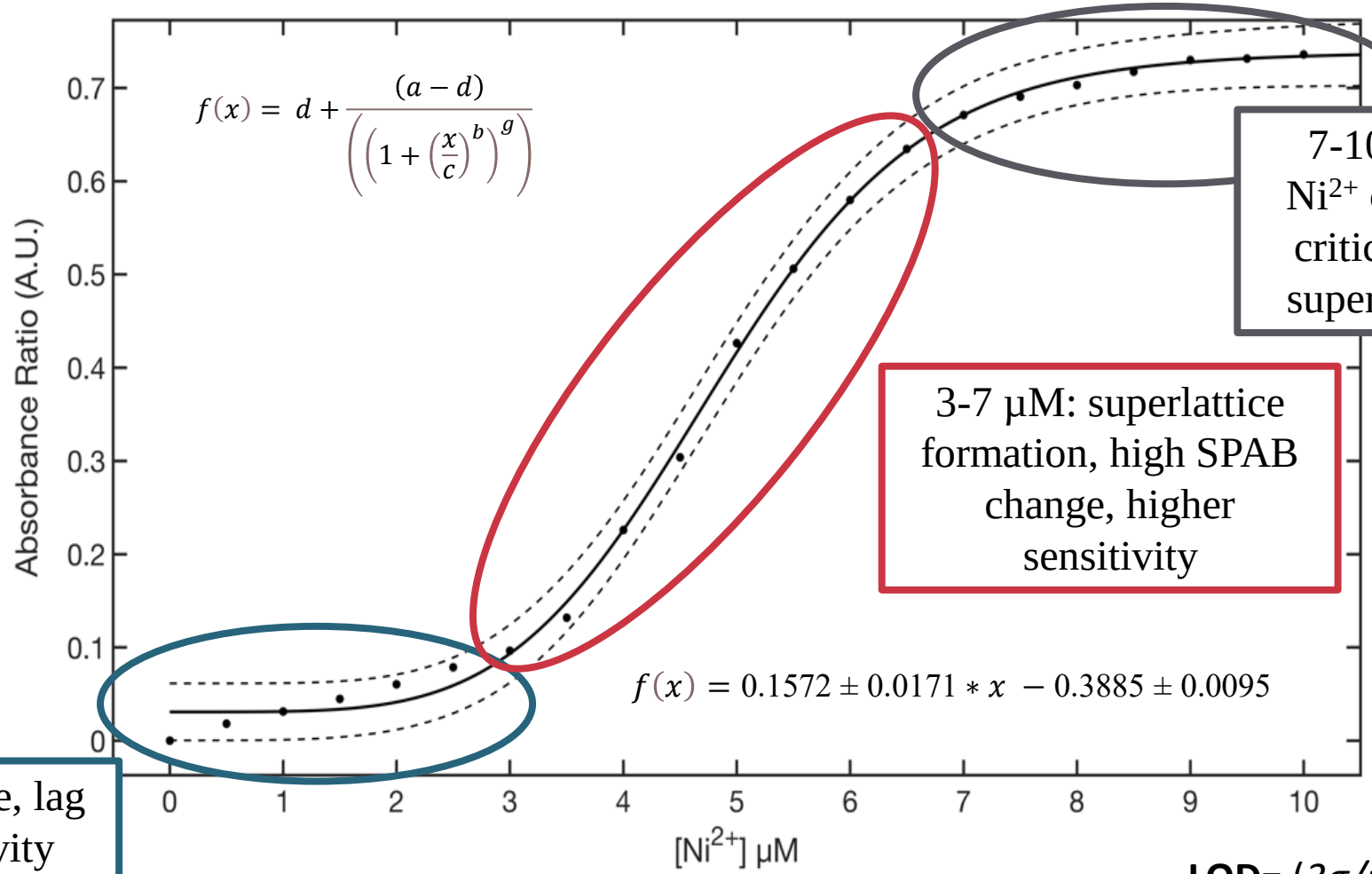

7-10 µM: the NPs-Ni^{2+} cluster reaches a critical mass and the superlattice collapses

3-7 µM: superlattice formation, high SPAB change, higher sensitivity

0-3 µM: small lattice, lag phase, low-sensitivity region

LOD= ($3\sigma/m$)= 2.15 µM

LOQ= ($10\sigma/m$)= 7.16 µM

Zannotti et al. Nanomaterials ***2021****, 11, 1733.*

How can the amount of functionalization affects the sensor results?

chemosensors

MDPI

Article

Optimizing the Heavy Metal Ion Sensing Properties of Functionalized Silver Nanoparticles: The Role of Surface Coating Density

Andrea Rossi [1], Massimiliano Cuccioloni [2,*], Lisa Rita Magnaghi [3], Raffaela Biesuz [3], Marco Zannotti [1,*], Laura Petetta [1], Mauro Angeletti [2] and Rita Giovannetti [1]

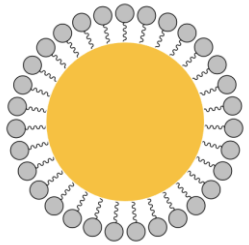

Full layer

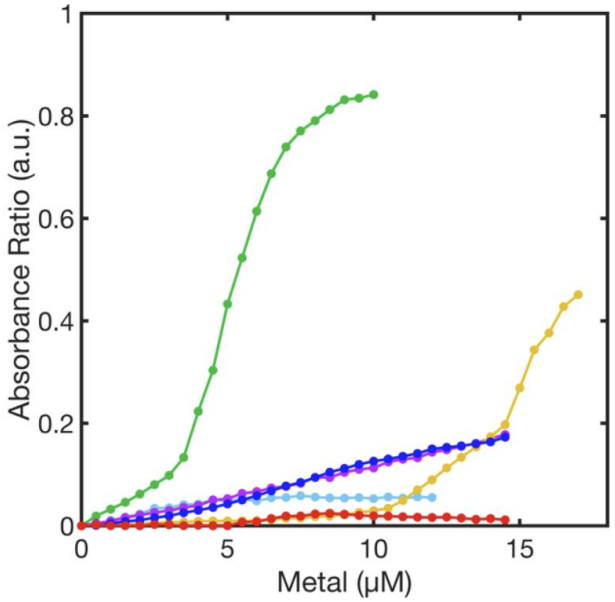

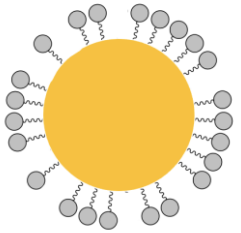

Partial layer 1

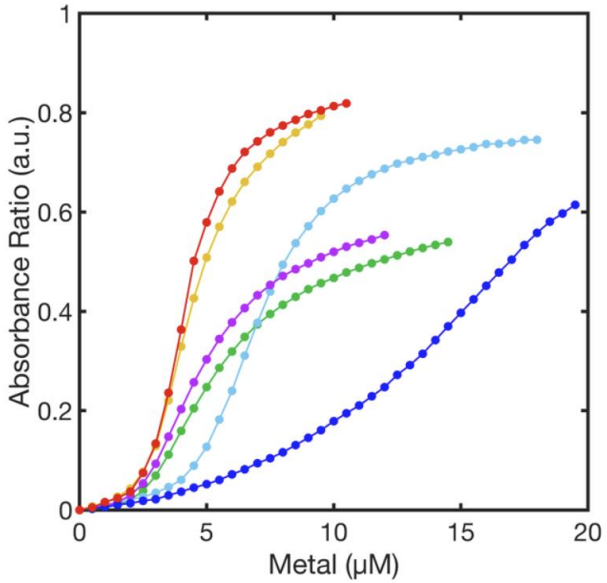

Zannotti et al. Chemosensors ***2022****, 10, 482.*

How can the amount of functionalization affects the sensor results?

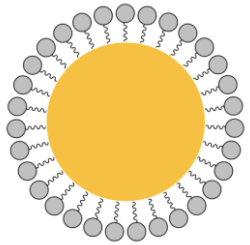

Full layer

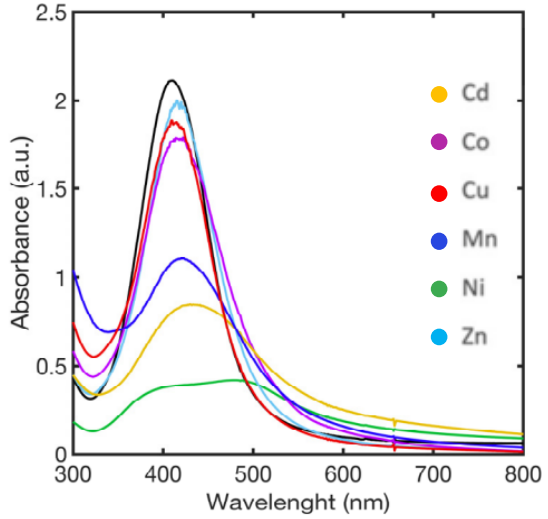

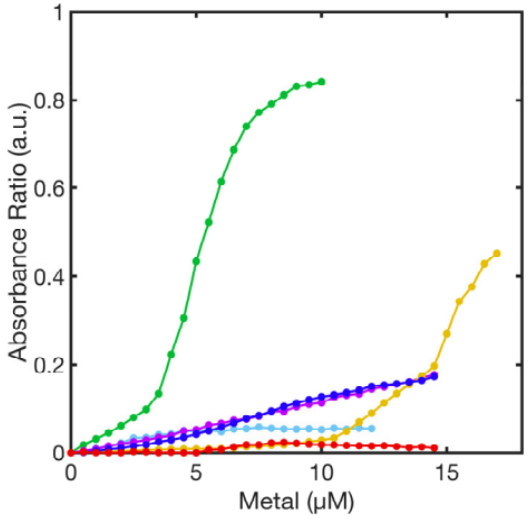

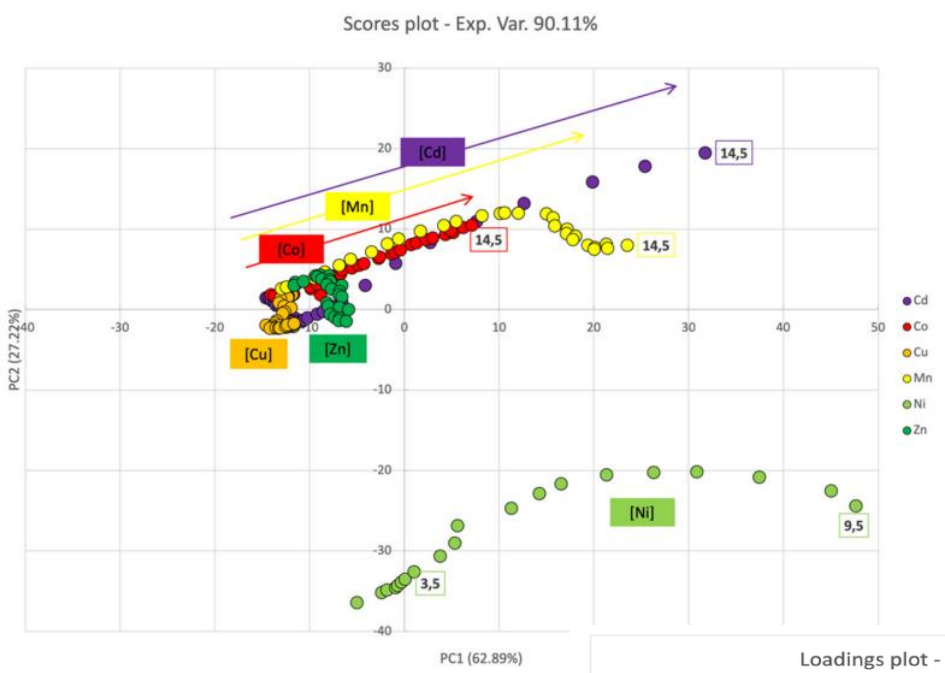

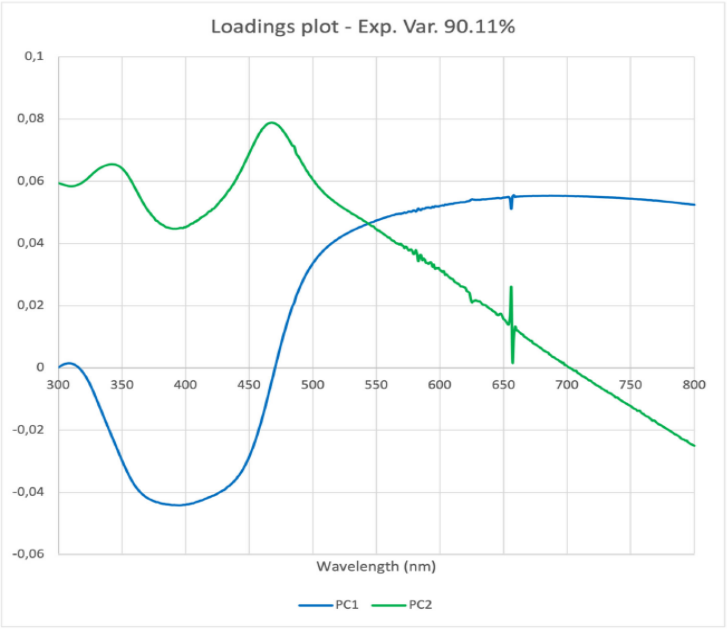

Chemistry Interdisciplinary Project

Zannotti et al. Chemosensors ***2022****, 10, 482.*

How can the amount of functionalization affects the sensor results?

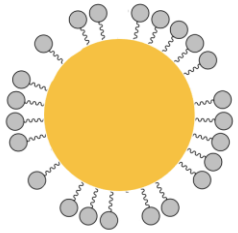

Partial layer 1

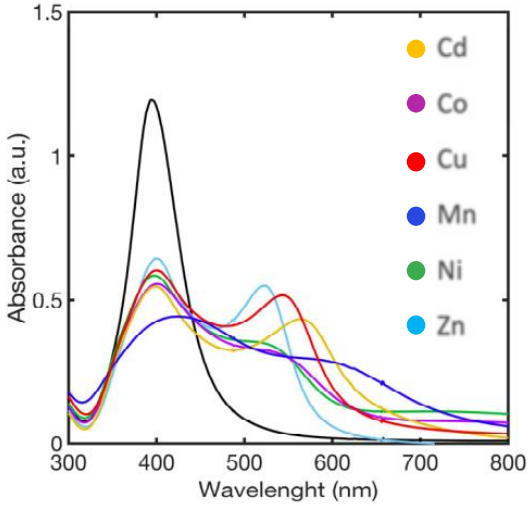

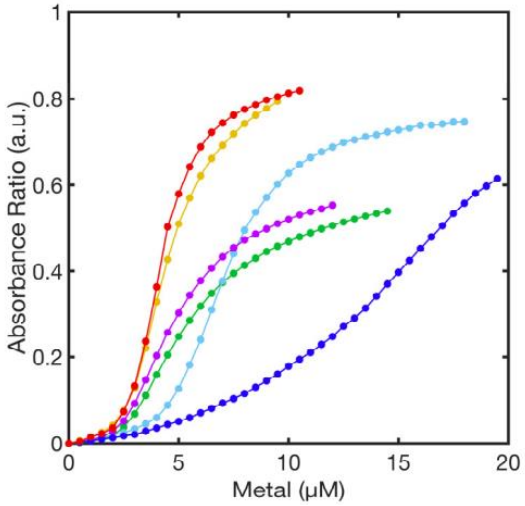

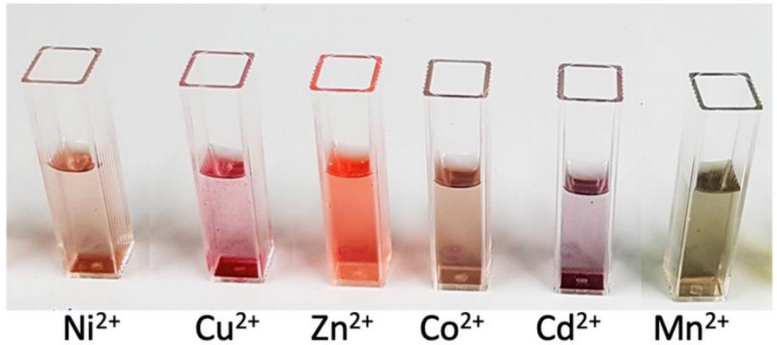

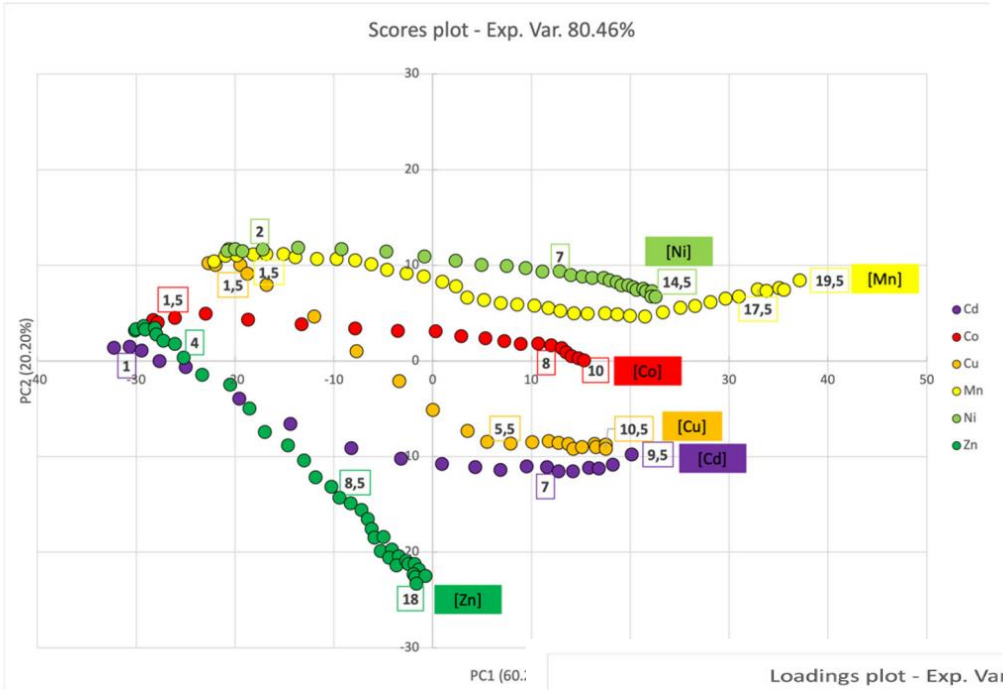

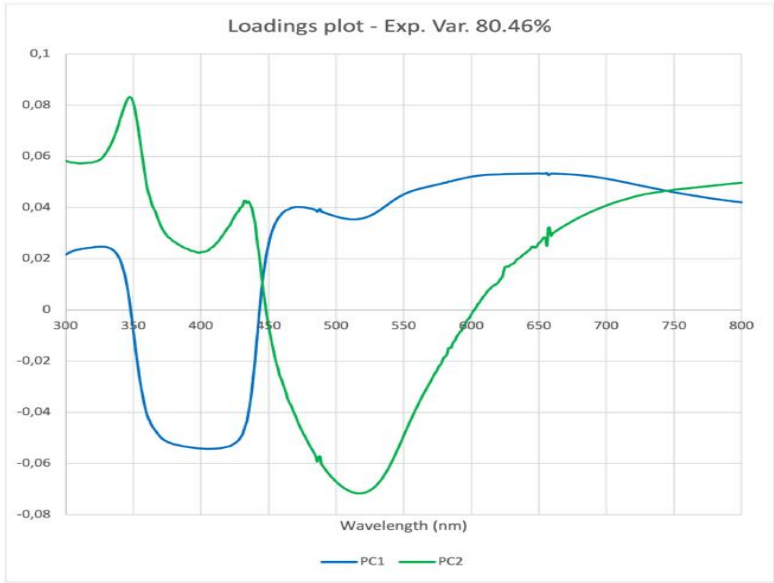

Zannotti et al. Chemosensors ***2022****, 10, 482.*

NANOMATERIALS: PHOTOCATALYSIS

Semiconductor photocatalytic technology has been demonstrated to be one of the "green" and effective strategies for solving environmental pollution problems.

Environmental photocatalysis, including water disinfection, hazardous waste remediation, air and water purification, deodorization, antibacterial, and self-cleaning has caused more and more attention in recent years.

New specific target pollutants
Industrial
Pharmaceutical
Agricultural
Human
Bacterial

High toxicity, health effect

Azo-dyes
Antraquinone dyes
Pesticidies

Pharmaceutics
Cyanobacterial toxins
Endocrine disruptors

2001: almost **400** papers

2020-2022: > **7000** papers

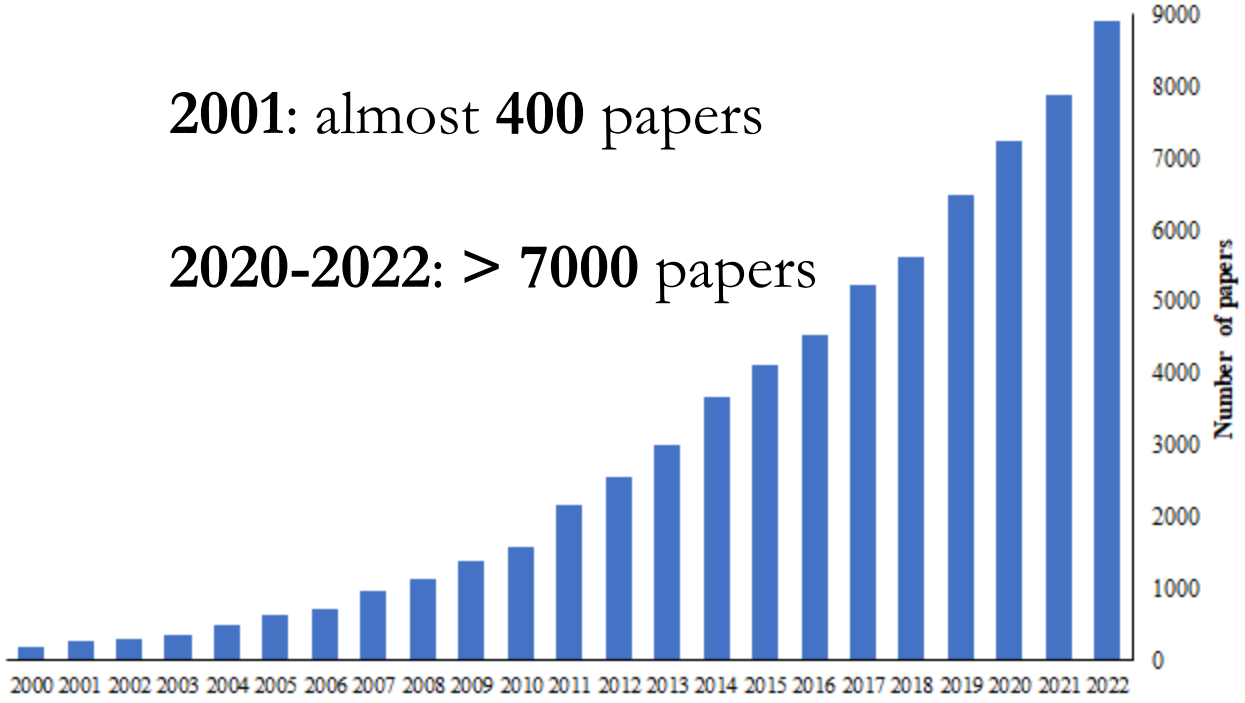

SCOPUS database: keywords "photocatal*" AND " degrad*"

FOUNDAMENTALS IN PHOTOCATALYSIS

Photocatalysis, as advanced oxidation process, have focused on the use of semiconductor materials as photocatalysts for environmental remediation, **TiO_2 is the most widely used as photocatalyst**.

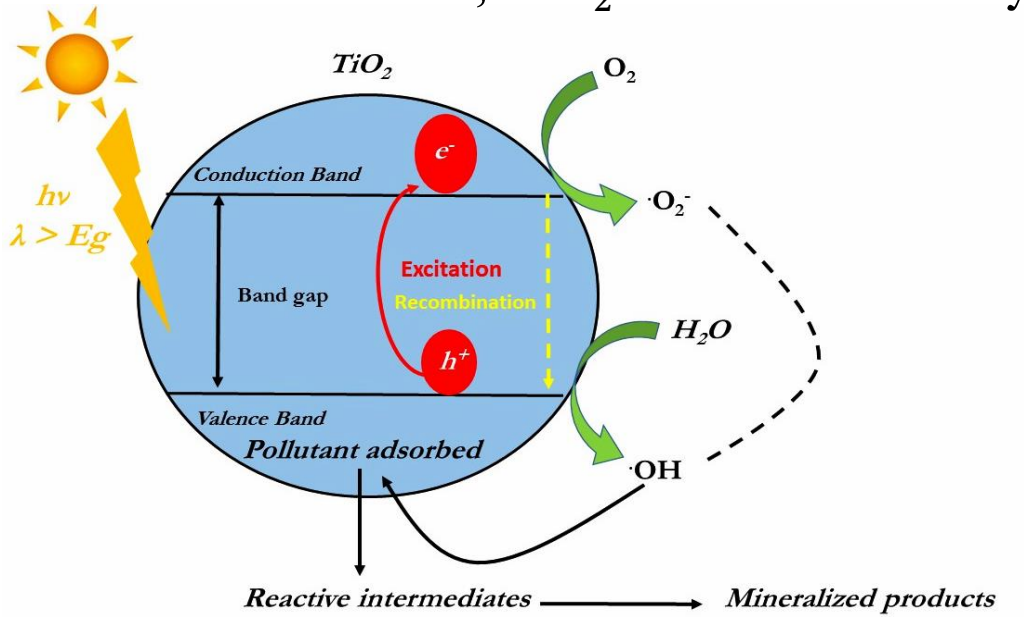

$$TiO_2 + h\nu\ (UV) \rightarrow TiO_2\,(e_{CB}^- + h_{VB}^+)$$

$$TiO_2\,(h_{VB}^+) + H_2O \rightarrow TiO_2 + H^+ + \cdot OH$$

$$TiO_2\,(h_{VB}^+) + OH^- \rightarrow TiO_2 + \cdot OH$$

$$TiO_2\,(e_{CB}^-) + O_2 \rightarrow TiO_2 + O_2^{\cdot -}$$

Oxidation of organic pollutants by the photogenerated-electron-related reactive oxygen species (ROS) such as hydroxyl (·OH) and superoxide ($O_2^{\cdot -}$) radicals

Narrow excitation wavelength : **large band gap energy (3.2 eV)**, important rate of recombination, a challenge is the modification of TiO_2 to improve the catalytic efficiency under visible solar radiation.

TiO_2 is active only under UV light (less than 5% of total incident solar spectrum), research has been focused on extending the light absorption of **TiO_2 under visible light**.

IMPROVEMENT OF TiO_2 PHOTOCATALYTIC PERFORMANCE

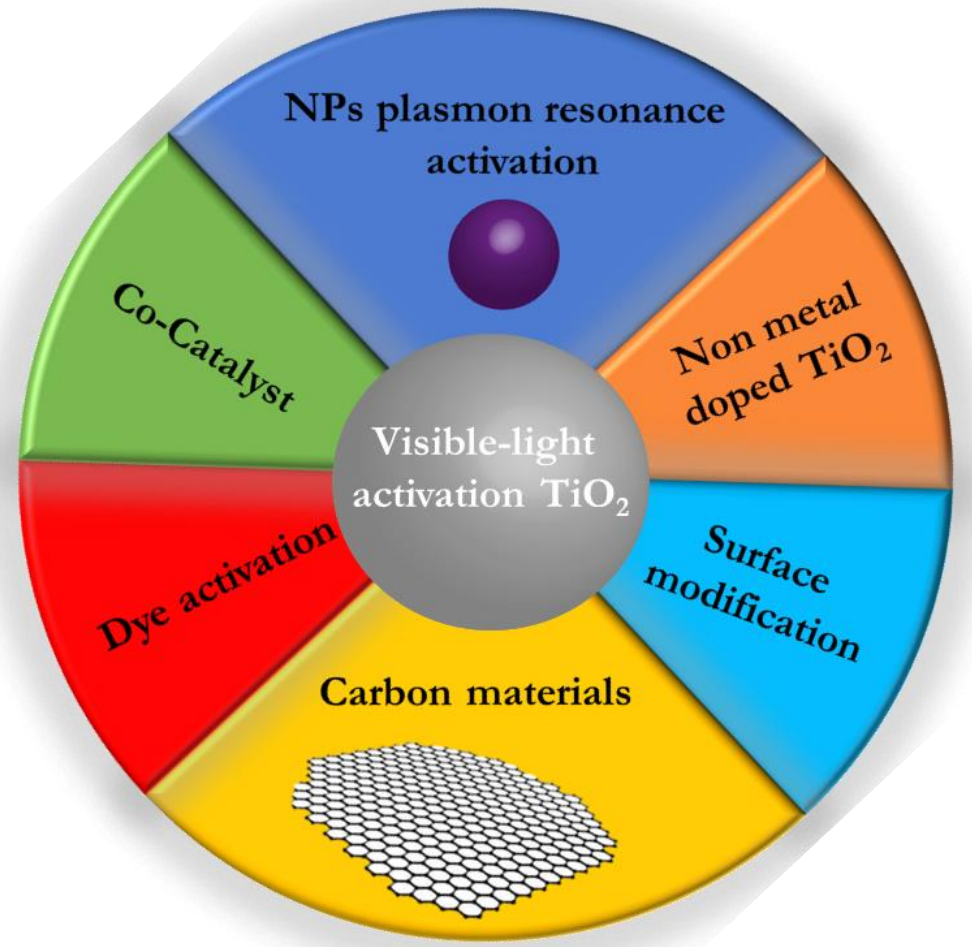

Modification of TiO_2 :

Noble metal nanoparticles/carbon materials/co-catalysts/dye/surface modifiers/ non metal

Visible light activation
Adsorption capacity improvement
Lowering band gap, Eg,
Simultaneous limitation of the electron-hole recombination rate

Visible light permits the use under solar light and an energy saving in terms of light source.

Nano-TiO_2 for dyes degradation in water

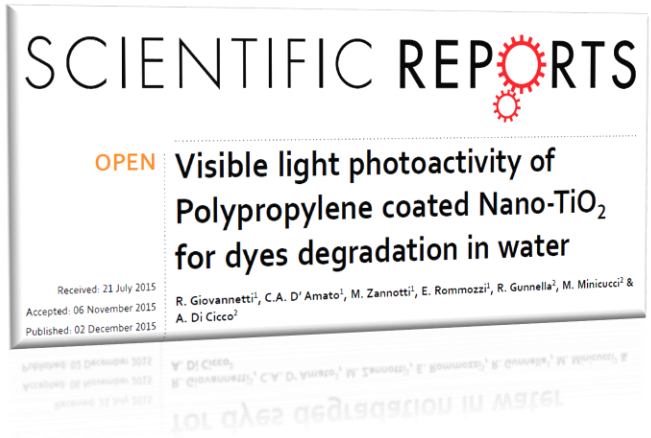
SCIENTIFIC REPORTS

OPEN

Visible light photoactivity of Polypropylene coated Nano-TiO_2 for dyes degradation in water

Received: 21 July 2015
Accepted: 06 November 2015
Published: 02 December 2015

R. Giovannetti[1], C.A. D' Amato[1], M. Zannotti[1], E. Rommozzi[1], R. Gunnella[2], M. Minicucci[2] & A. Di Cicco[2]

TiO_2 paste preparation for Anatase and Aeroxide P-25

- TiO_2 powder
- Acetylacetone
- Triton X-100
- Water

TiO_2 paste coated on PP strips

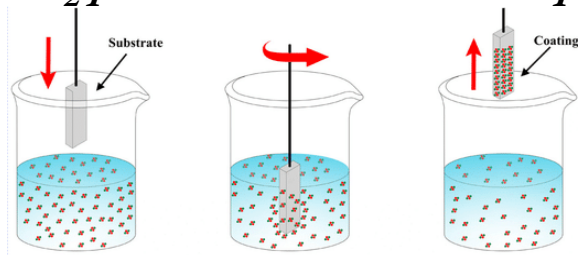

[PP@TiO_2] photocatalyst

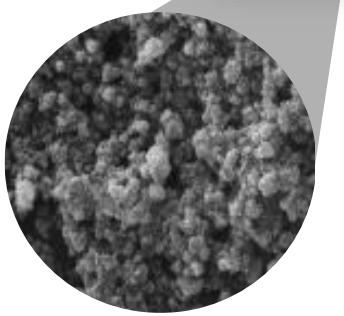

Photocatalytic Process

Adsorption

Photodegradation

Photocatalyst characterization

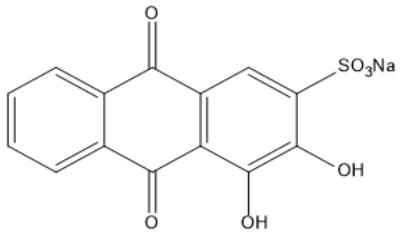

Alizarin Red S (ARS)

M. Zannotti et al. Scientific Reports **5**, *17801 (2016)*

UV-Vis spectral characterization of Alizarin Red-S

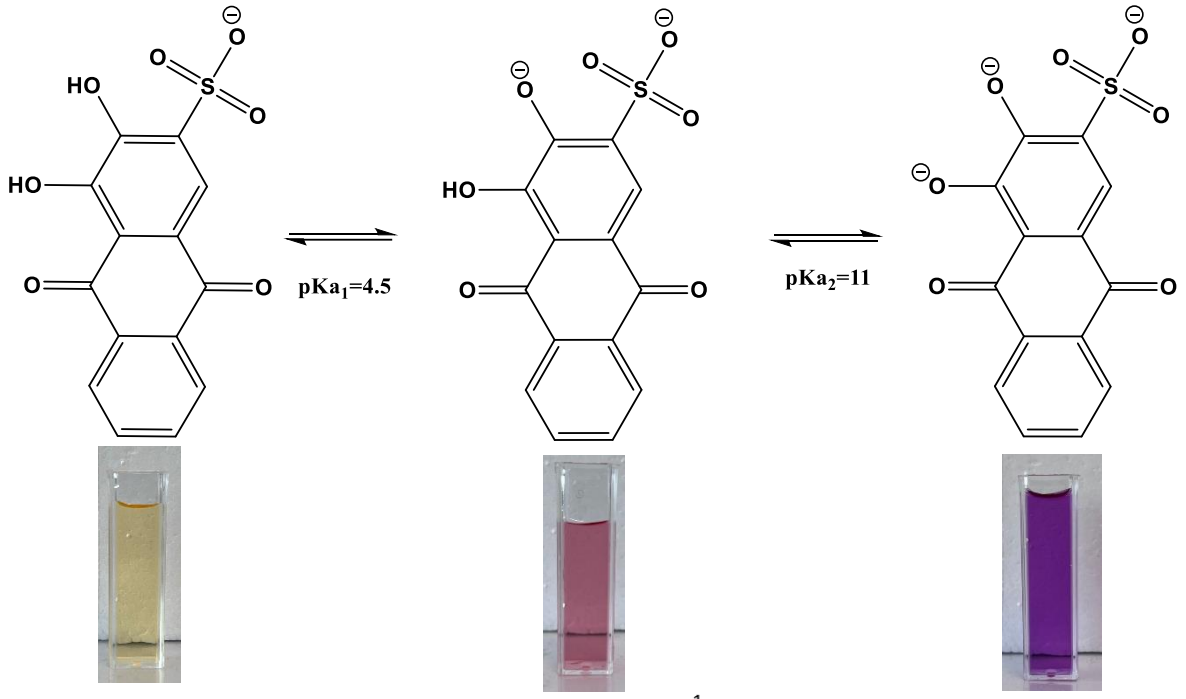

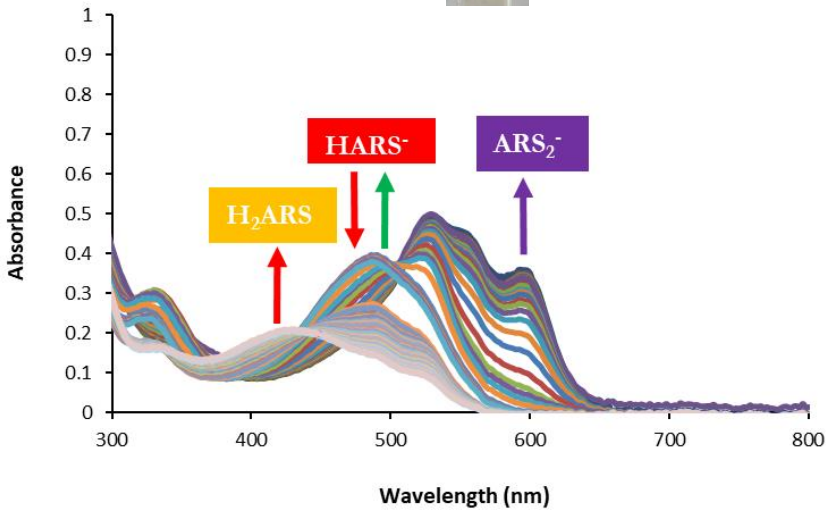

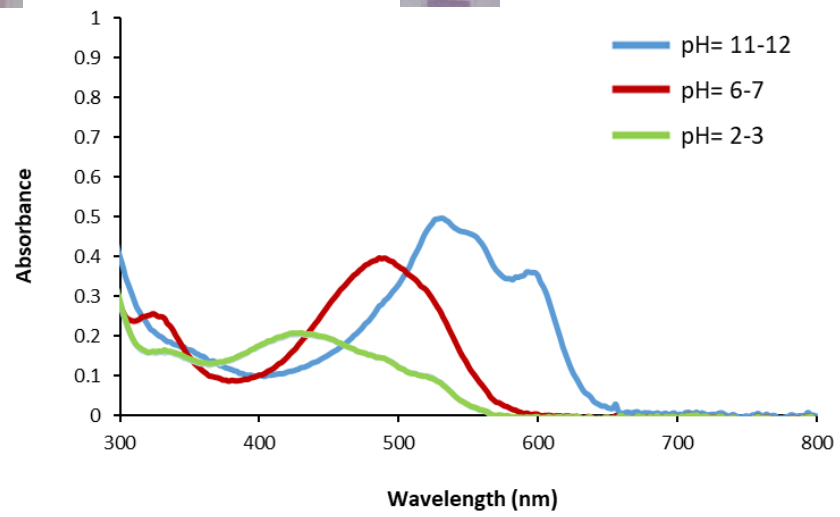

M. Zannotti et al. Scientific Reports **5,** *17801 (2016)*

Adsorption Study of Alizarin Red-S on PP@TiO_2 photocatalysts

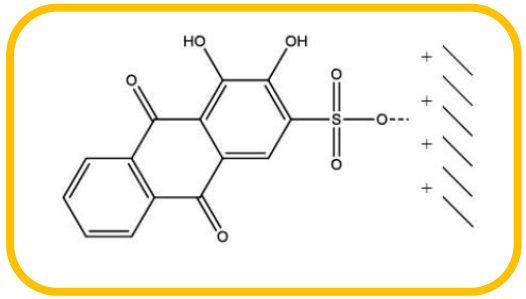

pH= 2

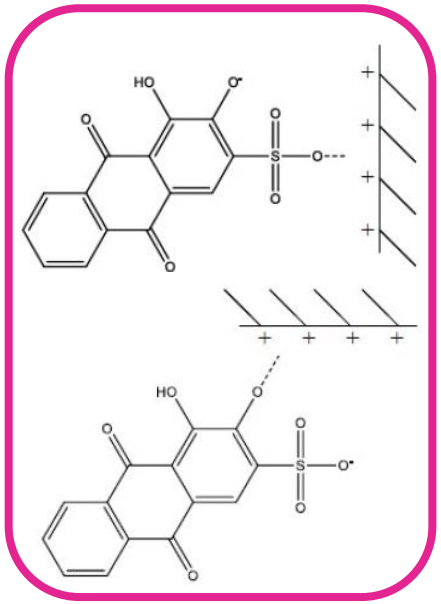

pH= 6

- **Acid pH**: **best** condition for **ARS adsorption**;
- At higher pH, steric hindrance and the presence of multiple anchoring sites can lead to competitive adsorption on TiO_2;

$$pH < pzc: Ti{-}OH + H^+ \Leftrightarrow TiOH_2^+$$

$$pH > pzc: Ti{-}OH + OH^- \Leftrightarrow TiO^- + H_2O$$

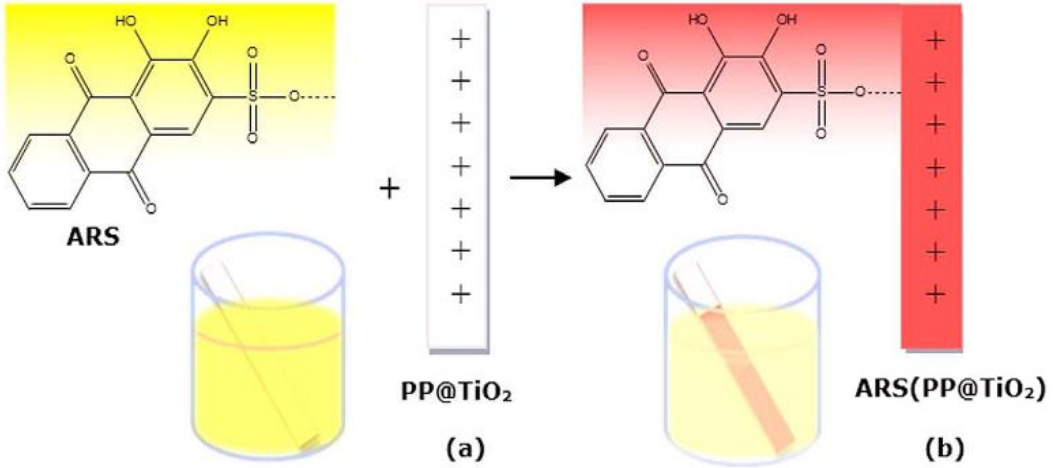

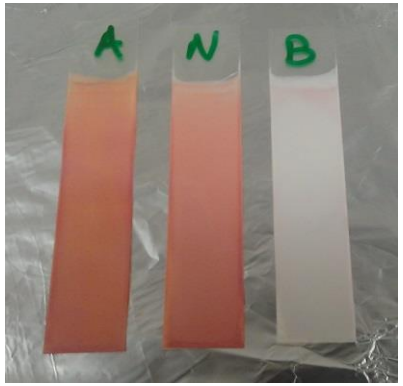

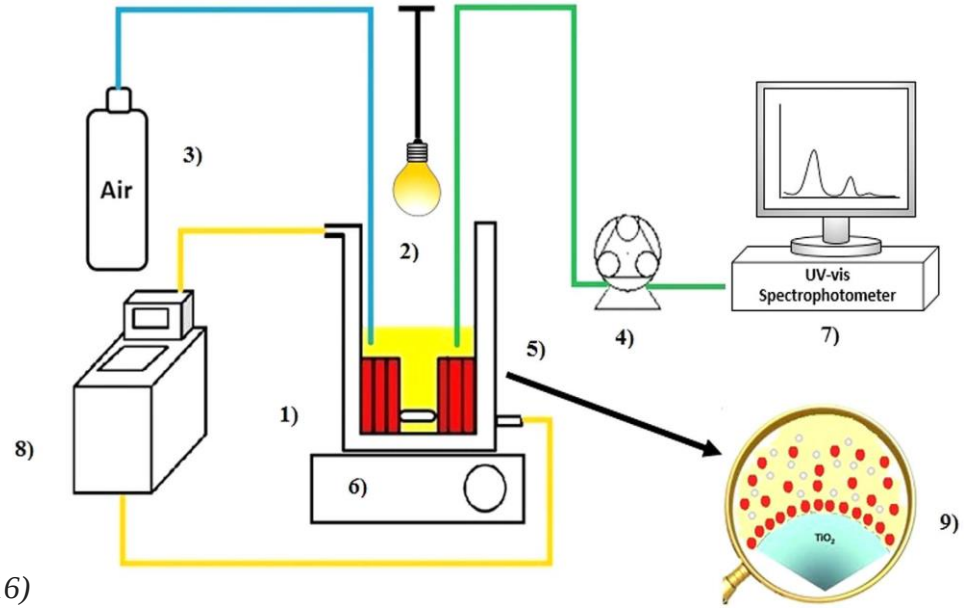

M. Zannotti et al. Scientific Reports **5**, *17801 (2016)*

Adsorption Study of Alizarin Red-S on PP@TiO_2 photocatalysts

The dye concentration influences the adsorption process

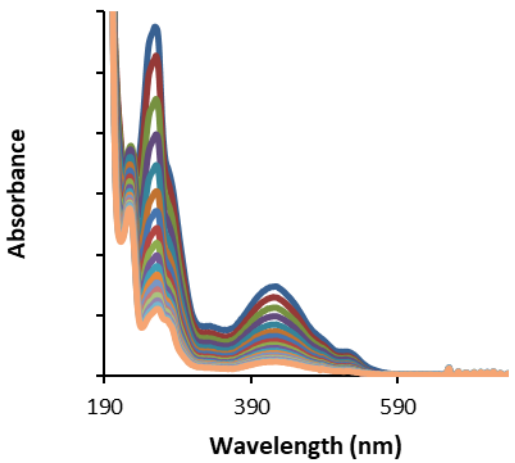

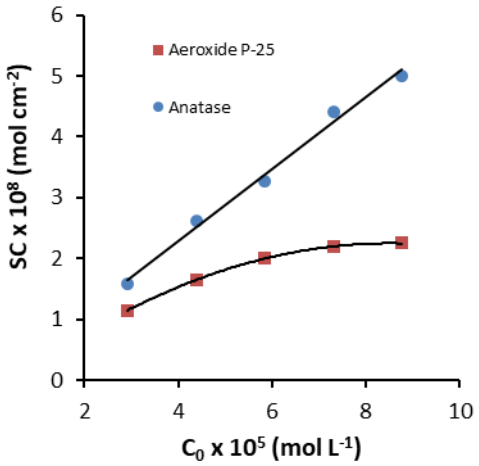

Equilibrium data

Anatase

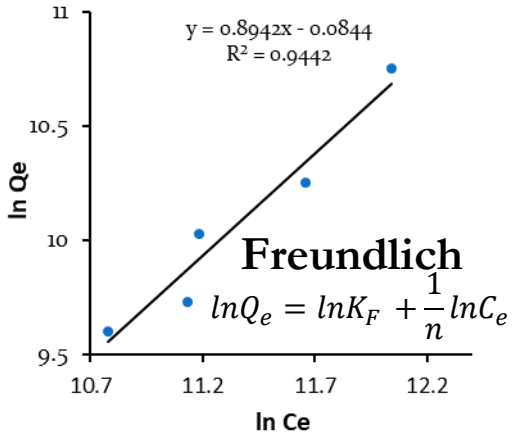

Aeroxide P-25

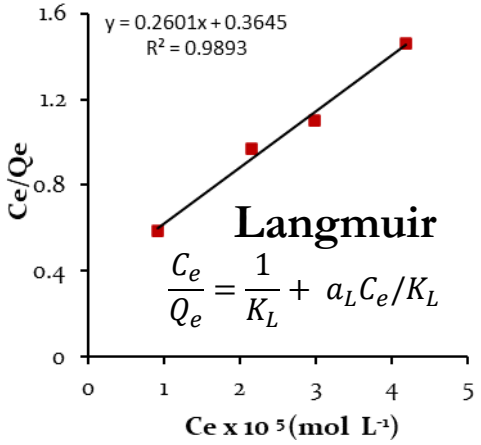

Multilayer adsorption

Monolayer adsorption

all dye molecules in the film have similar adsorption energy

Adsorption process follows pseudo-first order kinetic:

$$ln[(q_e - q_t)/q_e] = k_1 t$$

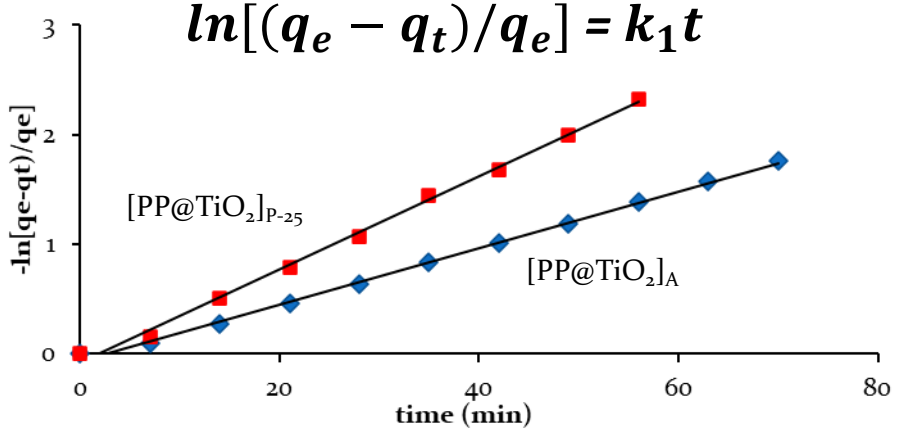

M. Zannotti et al. Scientific Reports **5,** *17801 (2016)*

Photodegradation of Alizarin Red-S by PP@TiO_2 photocatalysts

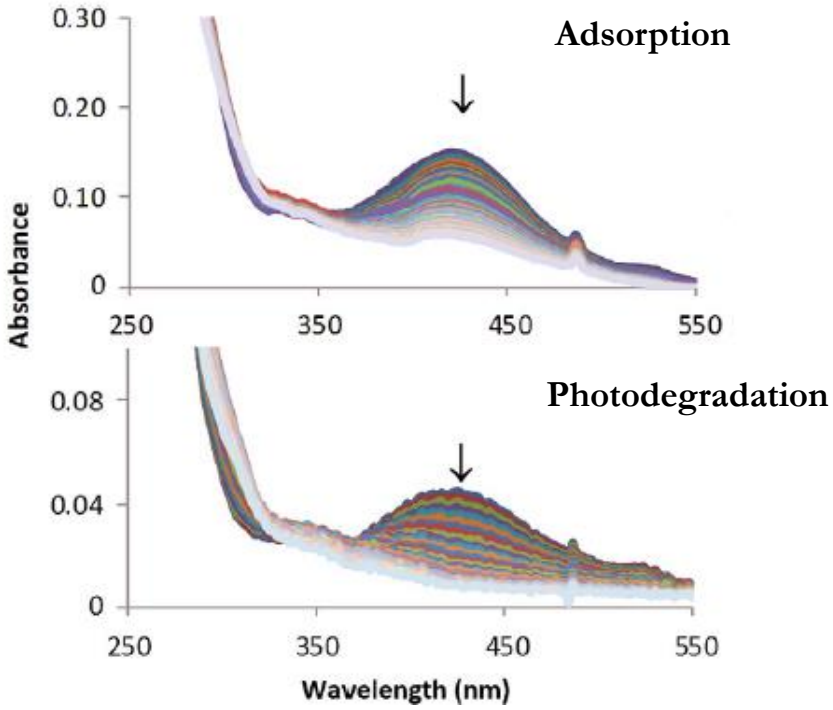

[ARS] (mol L^{-1})	k'_A (min^{-1})	[ARS] (mol L^{-1})	k'_{P-25} (min^{-1})
4.38×10^{-05}	$(2.11 \pm 0.03) \times 10^{-02}$	4.38×10^{-05}	$(1.55 \pm 0.03) \times 10^{-02}$
5.84×10^{-05}	$(1.23 \pm 0.02) \times 10^{-02}$	5.84×10^{-05}	$(0.67 \pm 0.02) \times 10^{-02}$
7.30×10^{-05}	$(0.65 \pm 002) \times 10^{-02}$	7.30×10^{-05}	$(0.33 \pm 0.02) \times 10^{-02}$

First order kinetic well describe the photodegradation process of [PP@TiO_2]

$$ln(C/C_0) = -k_2 t$$

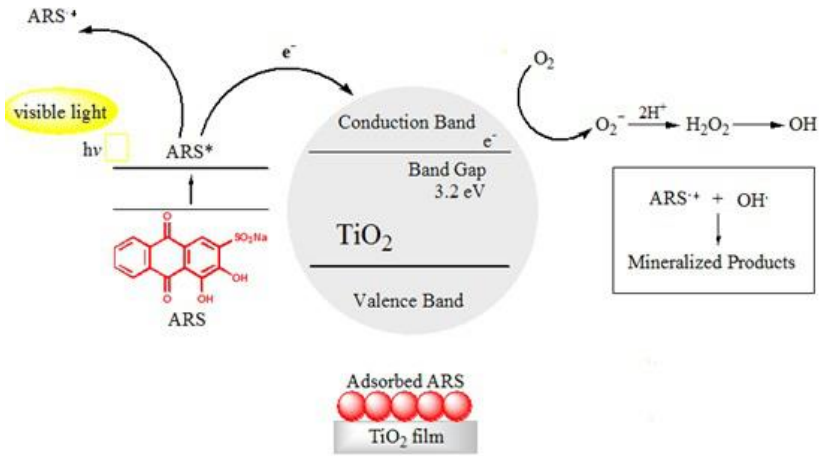

TiO_2 anatase shows the best results for ARS photodegradation as evidenced by the higher degradation constant and high absorption rate.

Chemistry Interdisciplinary Project

M. Zannotti et al. Scientific Reports **5,** *17801 (2016)*

Strategies to improve the photocatalytic activity of TiO_2 photocatalysts

Gold Nanoparticles modification to enhance visible light photoactivity

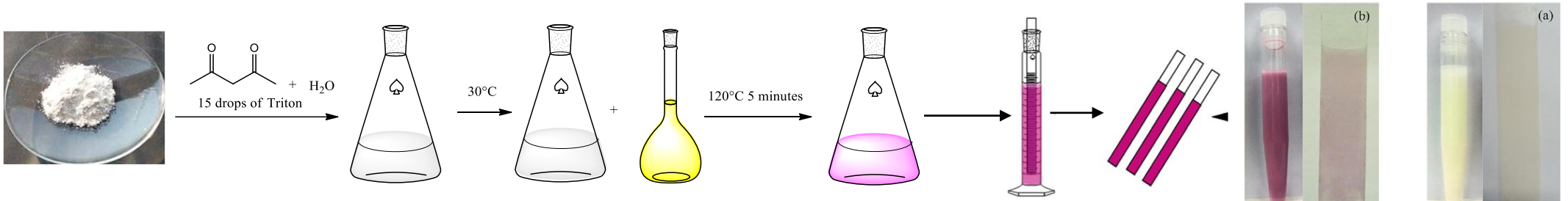

TiO_2 | $[TiO_2]_A$ paste | $HAuCl_4$ | TiO_2@AuNPs | $PP@Au\text{-}TiO_2]_A$ | $[PP@TiO_2]_A$


Contents lists available at ScienceDirect
Applied Surface Science
journal homepage: www.elsevier.com/locate/apsusc
ELSEVIER
Full Length Article

Enhancement of visible-light photoactivity by polypropylene coated plasmonic Au/TiO_2 for dye degradation in water solution

C.A. D'Amato [a,*], R. Giovannetti [a,*], M. Zannotti [a,*], E. Rommozzi [a], S. Ferraro [a], C. Seghetti [a], M. Minicucci [b], R. Gunnella [b], A. Di Cicco [b]

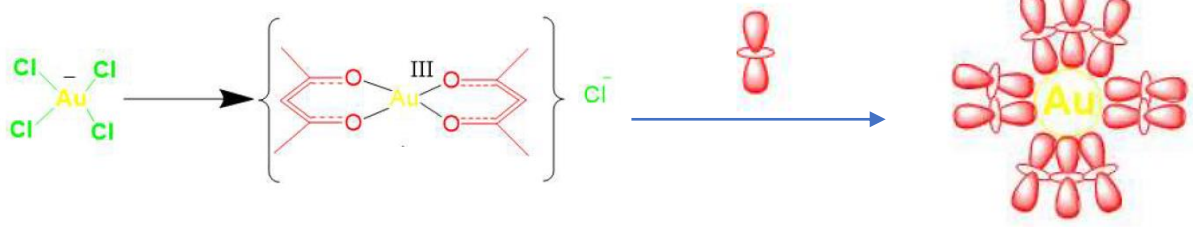

Strategies to improve the photocatalytic activity of TiO_2 photocatalysts

Characterization of PP@Au-TiO_2 photocatalyst

SEM

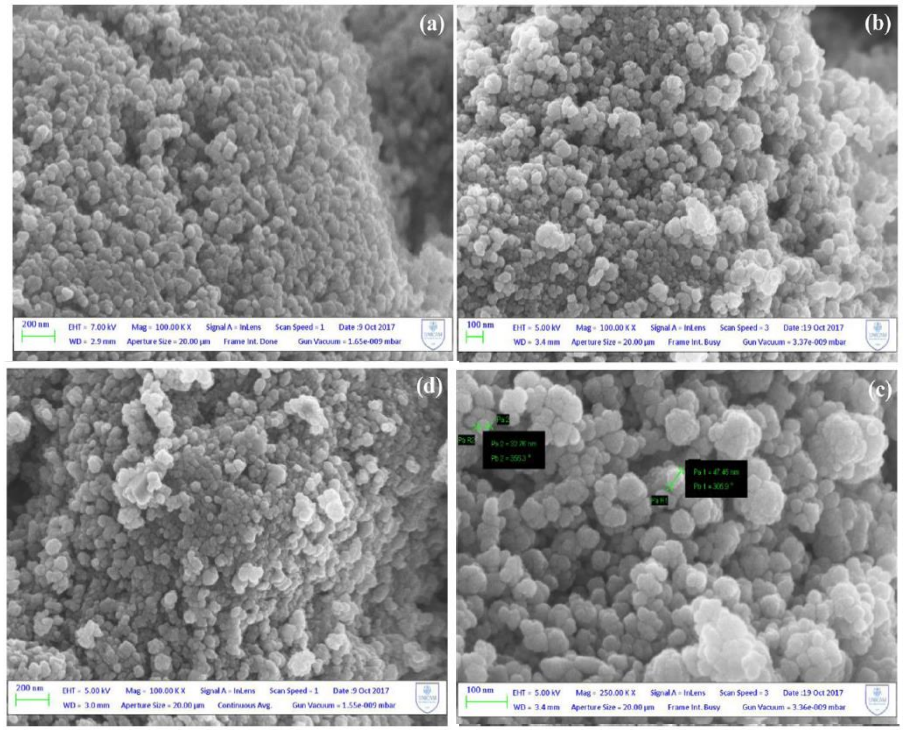

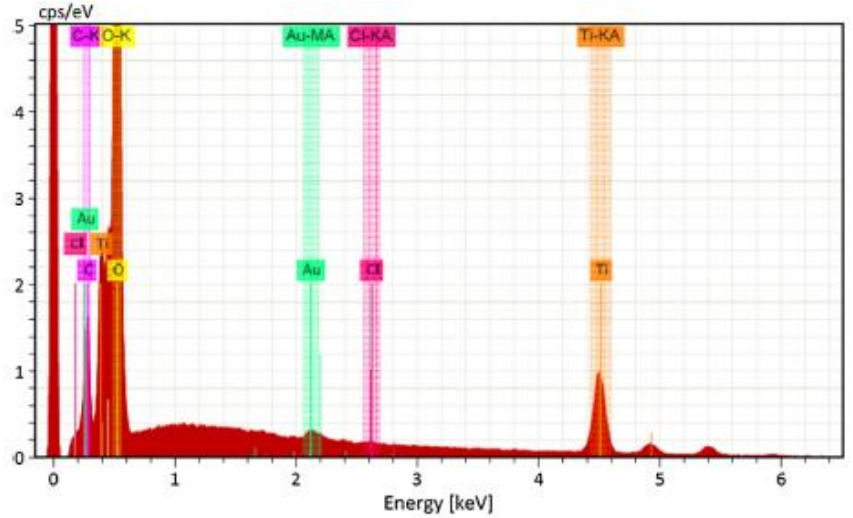

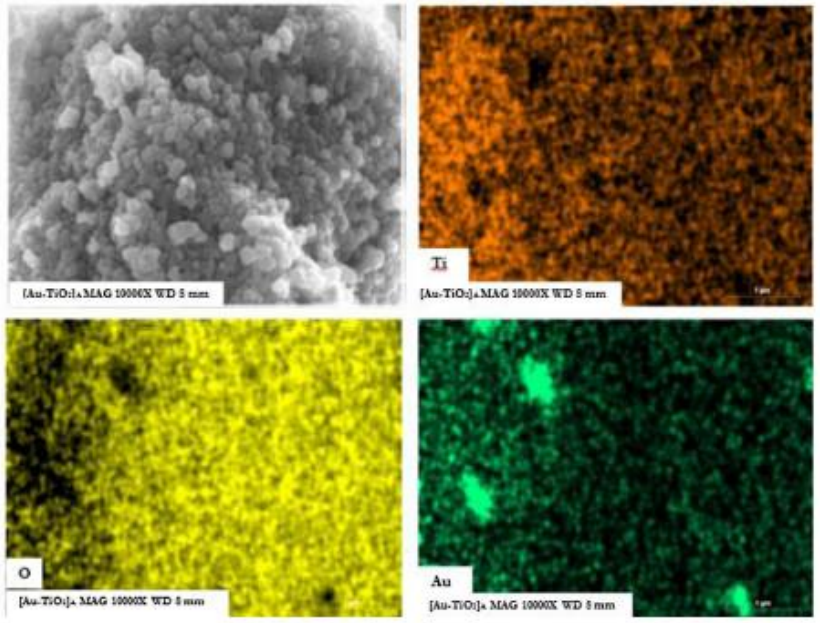

The **distribution maps** of elements show that **Ti, O and Au** cover all the surface area, with a greater evidence of Au on aggregates particles.

The growth of AuNPs directly inside the TiO_2 paste with **homogeneous distribution of gold on $[Au\text{-}TiO_2]_A$.**

Strategies to improve the photocatalytic activity of TiO_2 photocatalysts

Absorption and Photodegradation of ARS by PP@TiO_2

The adsorption process on $[PP@Au\text{-}TiO_2]_A$ was demonstrated to occur with **pseudo first order kinetic:**

$$ln[(q_e - q_t)/q_e] = k_1 t$$

The **photodegradation process** occurred with a rate described by the **first order kinetic:**

$$ln(C/C_0) = -k_2 t$$

$[PP@Au\text{-}TiO_2]_A$ showed an improvement in term of **photodegradation kinetics k_2** compared to that of **pure $[PP@TiO_2]_A$**

These results confirm the positive effect of AuNPs on TiO_2 paste.

	Gold wt.%	$HAuCl_4$ (mol/L)	$k_1 \times 10^2$ (min^{-1})	$k_2 \times 10^2$ (min^{-1})
$(PP@TiO_2)_A$	0	0	2.97	0.57
$(PP@Au\text{-}TiO_2)_A$	0.004	2.15×10^{-05}	3.08	0.63
$(PP@Au\text{-}TiO_2)_A$	0.006	3.24×10^{-05}	2.84	**1.40**
$(PP@Au\text{-}TiO_2)_A$	0.008	4.32×10^{-05}	2.91	**0. 97**
$(PP@Au\text{-}TiO_2)_A$	0.01	5.40×10^{-05}	3.56	0.74

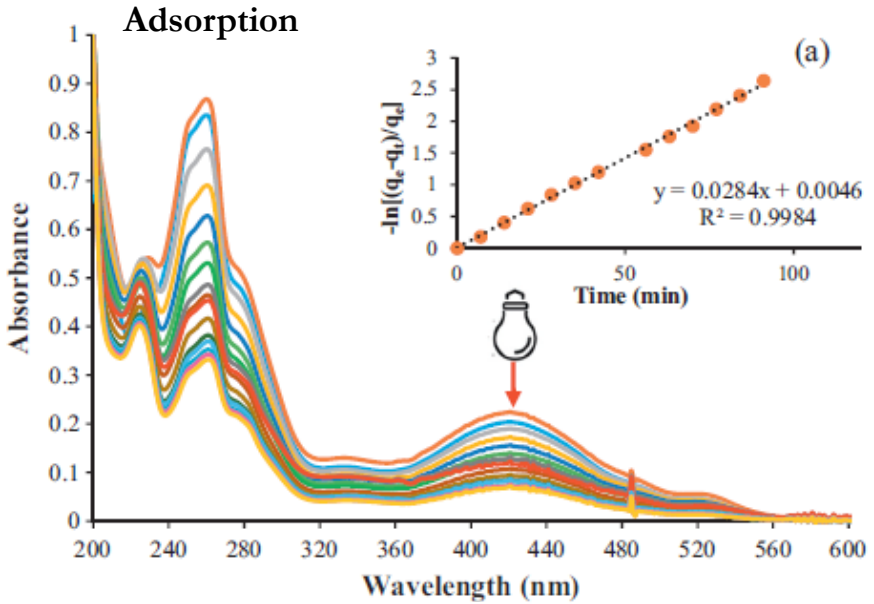

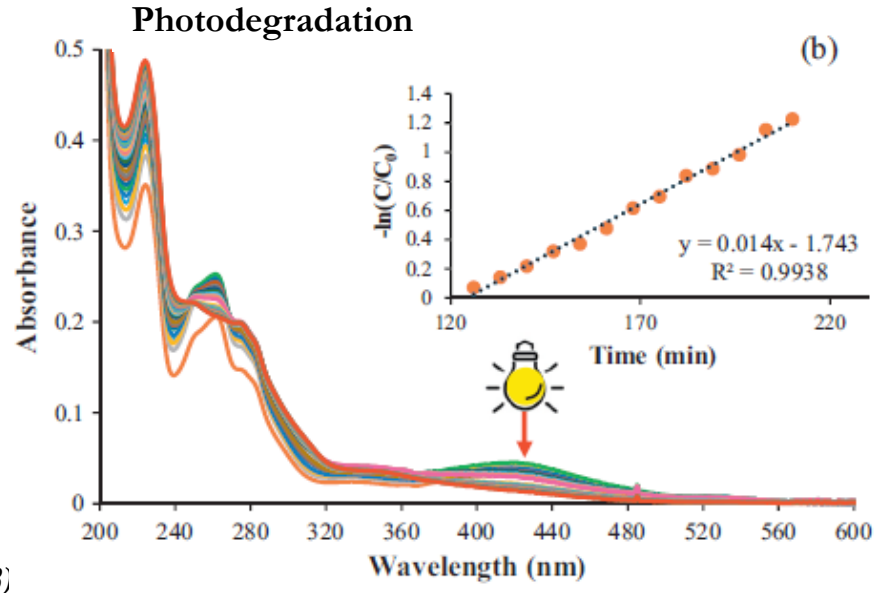

M. Zannotti et al. Applied Surface Science 441 (2018)

Strategies to improve the photocatalytic activity of TiO_2 photocatalysts

Surface modification with Ascorbic Acid (AA)

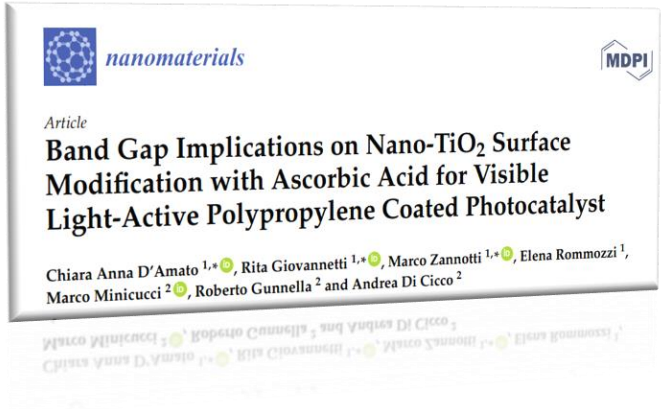

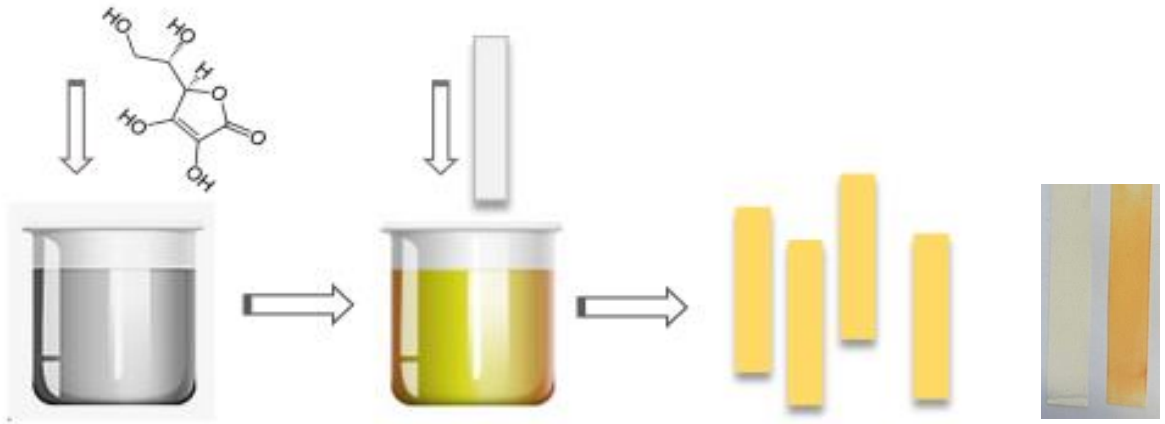

$[TiO_2]_A$ paste $[AA\text{-}TiO_2]_A$ paste $[PP@AA\text{-}TiO_2]_A$

Strategies to improve the photocatalytic activity of TiO_2 photocatalysts

Photodegradation of ARS by PP@AA-TiO_2 photocatalyst

PL Spectra

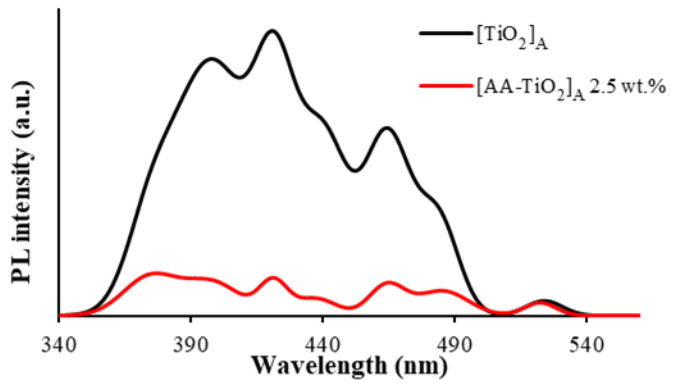

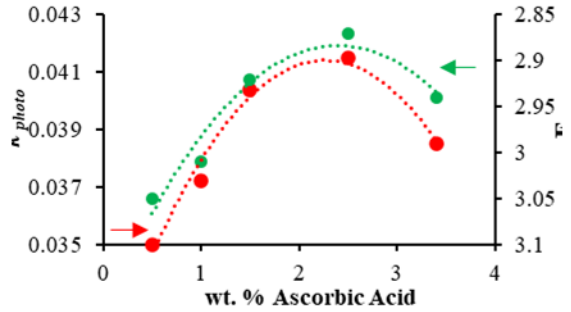

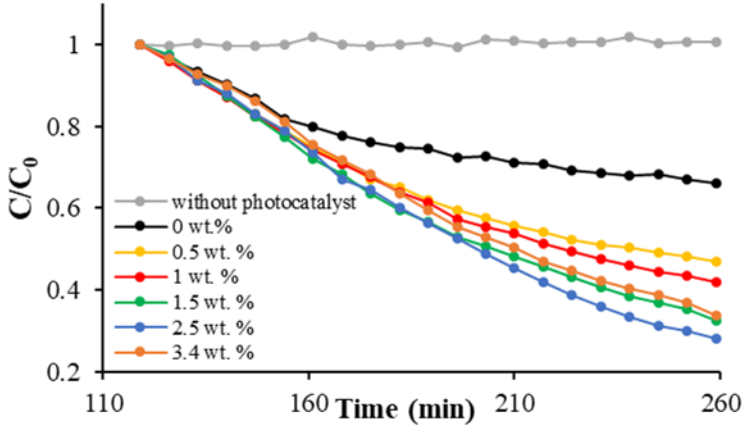

M. Zannotti et al, Nanomaterials MDPI ***2018****, 8, 599*

DRS spectra

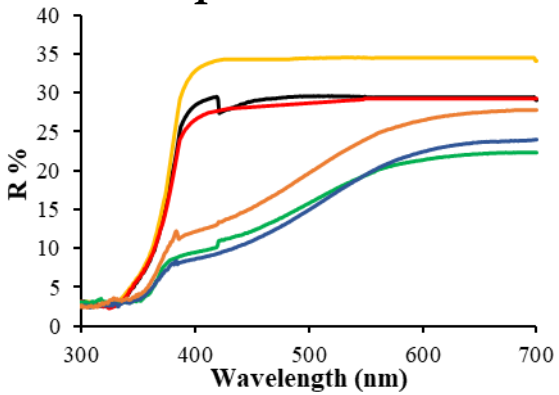

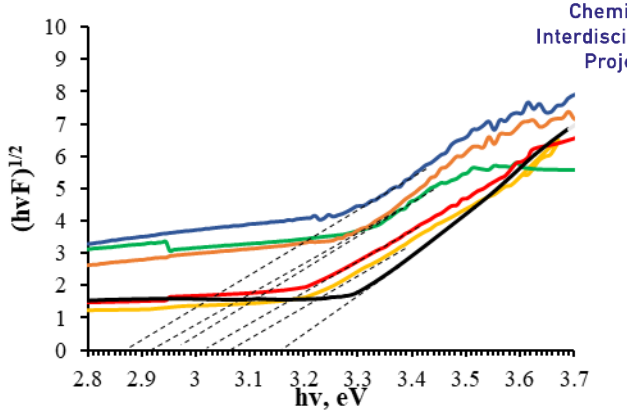

E_g, k_{ads} and k_{photo} values for [PP@AA-TiO_2]$_A$ containing different AA wt. %.

AA wt. %	E_g (eV)	$10^2 k_{ads}$ (min^{-1})	$10^2 k_{photo}$(min^{-1})
0	3.15	3.75	1.99
0.5	3.05	3.55	3.50
1	3.01	3.47	3.72
1.5	**2.92**	**3.46**	**4.04**
2.5	**2.87**	**3.18**	**4.15**
3.4	2.94	3.09	3.85

- PL spectra indicate a **suppression of electron-hole recombination** process in presence of AA
- Dye adsorption follow the **Langmuir model**, instead the results obtained with the non-modified photocatalyst: $lnQe = lnK_F + 1/n\ lnCe$
- Dye adsorption follows a **pseudo first order kinetics** $ln[(q_e - q_t)/q_e = k_{ads}\ t$
- K_{ads} linearly decreased with increasing amount of AA wt.%, however increasing AA amount corresponds to a lowering Eg, with a better photocatalytic performance **(BEST 2.5 wt.%)**

Strategies to improve the photocatalytic activity of TiO_2 photocatalysts

Based-Graphene TiO_2 photocatalyst to improve photocatalytic activity

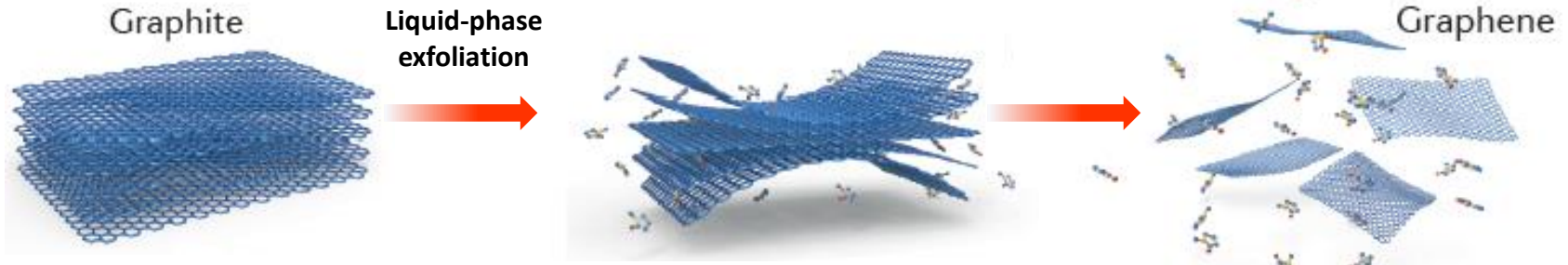

Chemistry Interdisciplinary Project

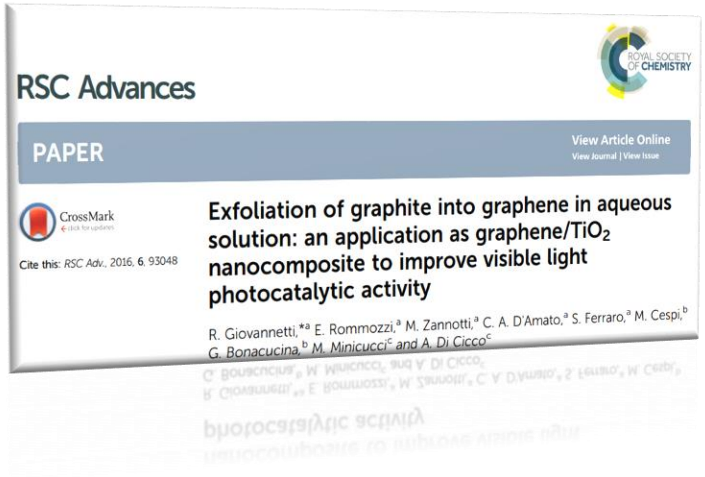
RSC Advances

PAPER

View Article Online

Exfoliation of graphite into graphene in aqueous solution: an application as graphene/TiO_2 nanocomposite to improve visible light photocatalytic activity

R. Giovannetti,*[a] E. Rommozzi,[a] M. Zannotti,[a] C. A. D'Amato,[a] S. Ferraro,[a] M. Cespi,[b] G. Bonacucina,[b] M. Minicucci[c] and A. Di Cicco[c]

Cite this: *RSC Adv.*, 2016, 6, 93048

Graphene dispersion preparation

Exfoliation of Graphite by ultrasonic treatment in presence of surfactant Triton X-100.

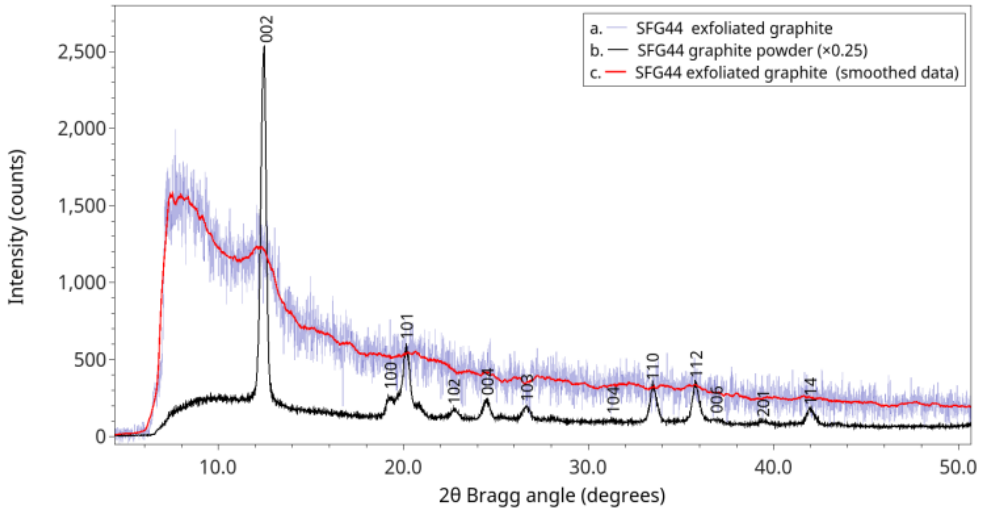

Graphene nanomaterials: large specific area, flexible structure, extraordinary mobility of charge carriers at room temperature, high thermal and electrical conductivities, high chemical stability; act as visible light absorbers and electron acceptor.

Strategies to improve the photocatalytic activity of TiO_2 photocatalysts

Photodegradation of ARS using exfoliated graphene-TiO_2 photocatalyst

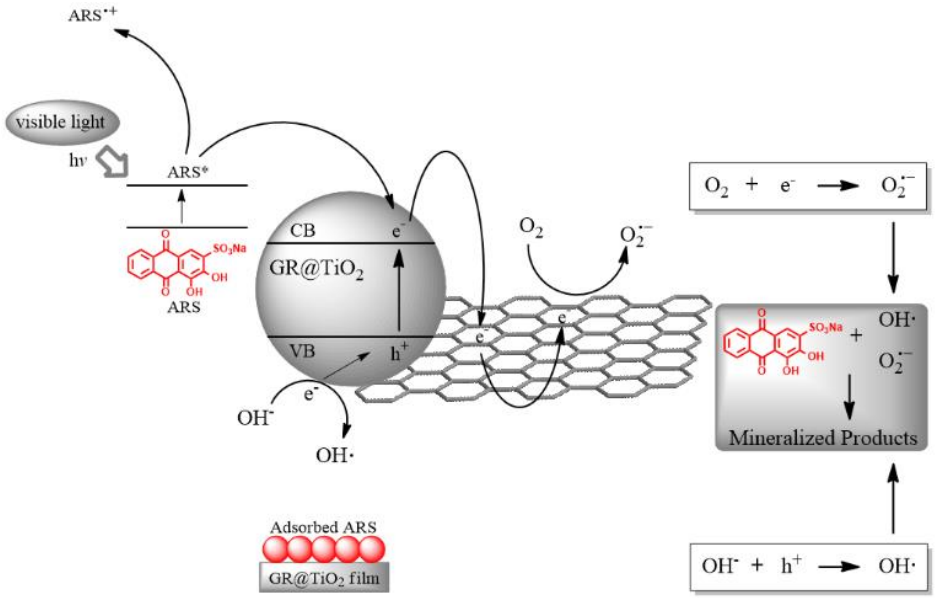

- Different concentrations of as preparaed GR used to modify $[TiO_2]_A$
- Adsorption process follows the **Freundlich model**: **multilayer absorption** mechanism as for $[TiO_2]_A$;
- **GR influences positively the absorption kinetics** of ARS respect to pure TiO_2, but k_{ads} are very similar for all the catalysts with GR;
- Increasing GR amount the **adsorbed concentration increases** due to **π-π interactions**;
- Photodegradation efficiency increases with GR as demonstrated by the increasing of the ***k_{photo}***

Photogenerated electrons are transferred on GR(electron acceptor) inhibiting the electron-hole recombination.

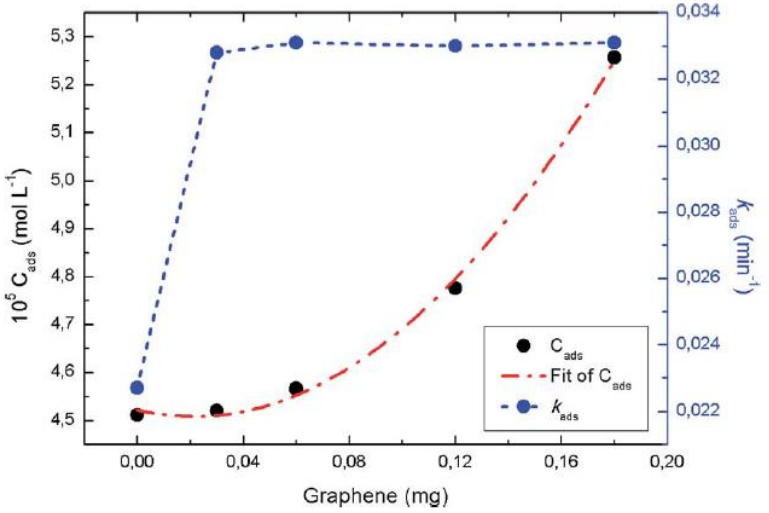

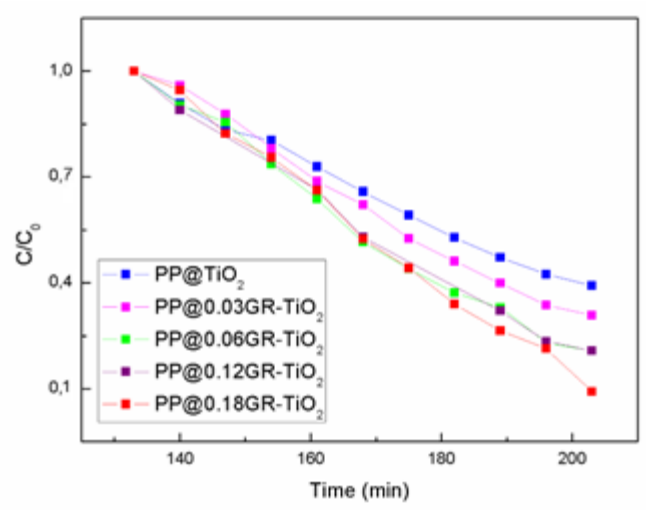

k_{ads} and k_{photo} with various catalysts

Catalyst name mgGR@TiO_2	$k_{ads} \times 10^2$ (min^{-1})	Adj. R_{ads}^2	$k_{photo} \times 10^3$ (min^{-1})	Adj. R_{photo}^2
PP@TiO_2	2.54	0.9967	7.70	0.9960
PP@0.03GR–TiO_2	3.28	0.9981	9.70	0.9949
PP@0.06GR–TiO_2	3.31	0.9966	11.56	0.9920
PP@0.12GR–TiO_2	3.30	0.9986	11.26	0.9924
PP@0.18GR–TiO_2	3.31	0.9996	12.53	0.9939

Strategies to improve the photocatalytic activity of TiO_2 photocatalysts

Based-Graphene TiO_2 photocatalyst to improve photocatalytic activity

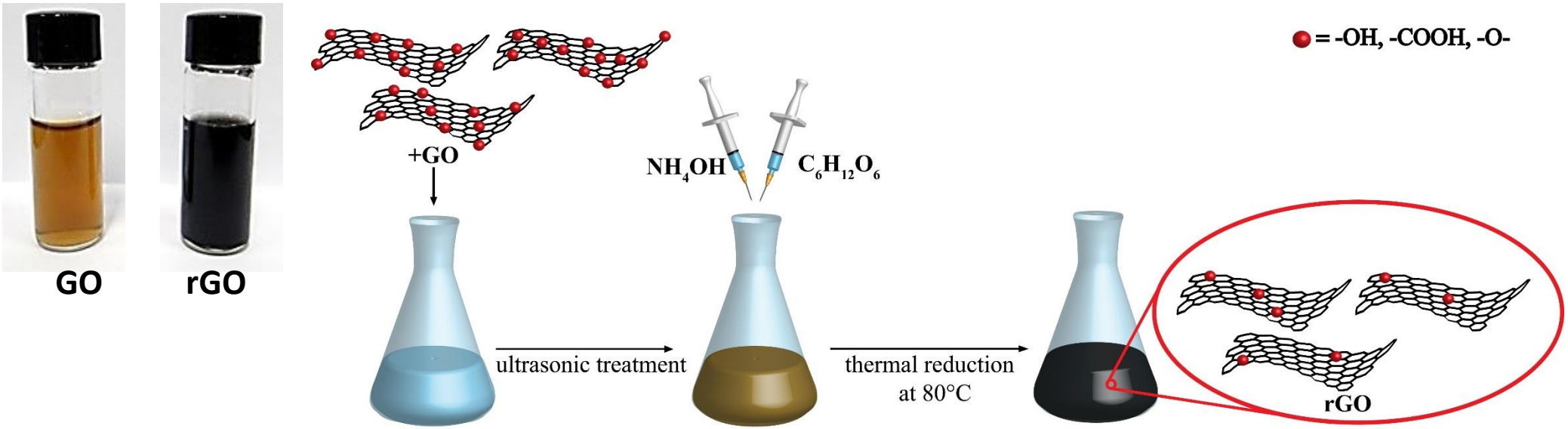

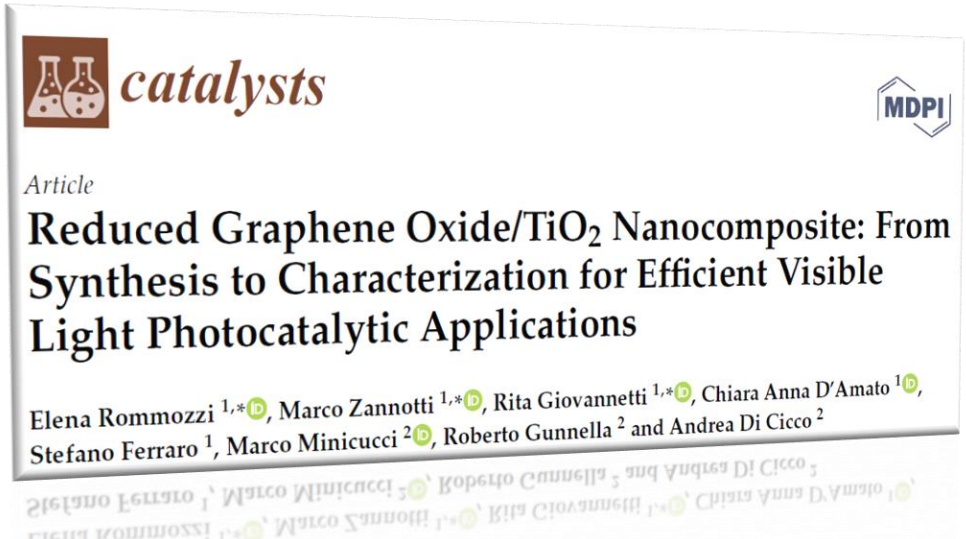

catalysts

MDPI

Article

Reduced Graphene Oxide/TiO_2 Nanocomposite: From Synthesis to Characterization for Efficient Visible Light Photocatalytic Applications

Elena Rommozzi [1,*], Marco Zannotti [1,*], Rita Giovannetti [1,*], Chiara Anna D'Amato [1], Stefano Ferraro [1], Marco Minicucci [2], Roberto Gunnella [2] and Andrea Di Cicco [2]

3.2) Synthesis of Reduced-Graphene Oxide (rGO)

Green reduction of Graphene Oxide by using glucose as reducing agent at 80°C.

Strategies to improve the photocatalytic activity of TiO_2 photocatalysts

Based rGO-TiO_2 as photocatalyst for the degradation of Alizarin Red-S

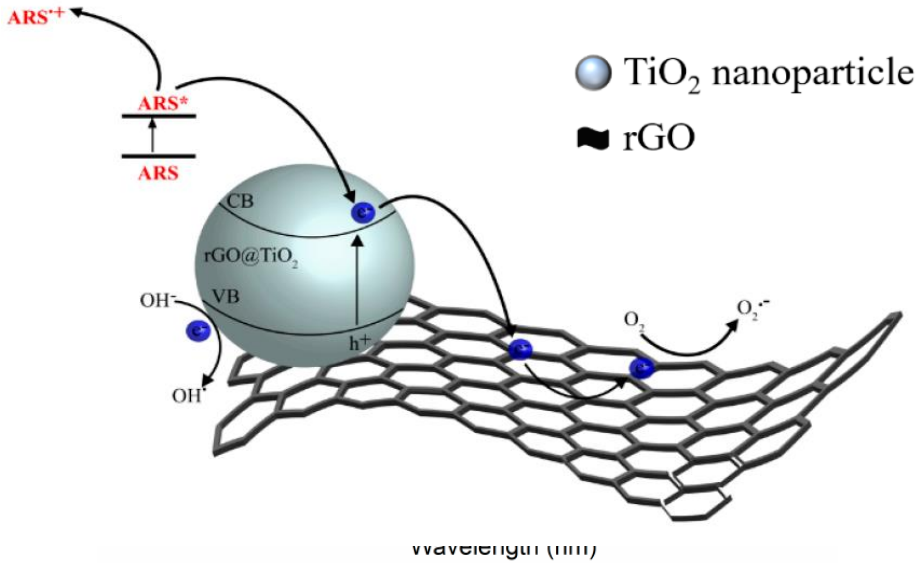

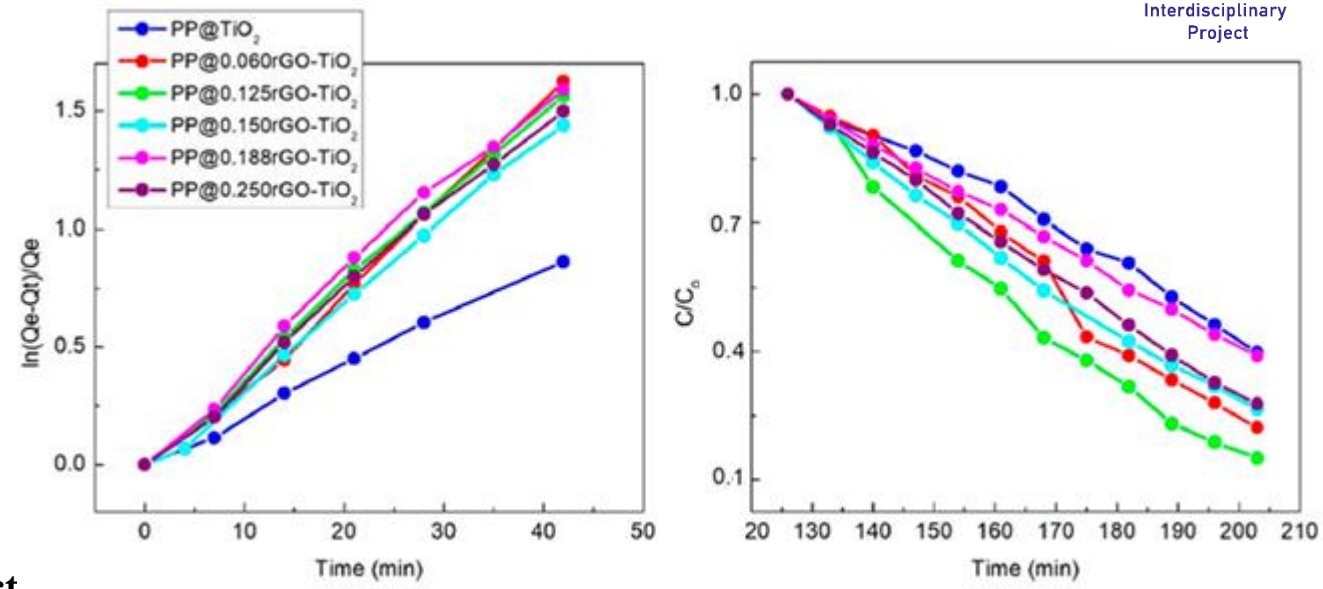

- **PL intensity of PP@rGO-TiO_2 decrease with respect to pure TiO_2,** demonstrating an efficient **recombination reduction** between electrons and holes;
- Work function of graphene is 4.42 eV, TiO_2 CB is around 4.21 eV, rGO can accept the photogenerated electrons from TiO_2, with effective charge carrier separation;
- All the **k_{ads} increase** with the modified **rGO-TiO_2** paste, are higher with respect to pure-TiO_2 paste;
- **First order kinetic** well describes the **photodegradation** steps, best performance obtained by using **PP@0.125rGOTiO$_2$ (higher k_{photo}).**

k_{ads} and k_{photo} values with R^2 for all photocatalysts.

Catalyst Name	$k_{ads} \times 10^2$	R^2_{ads}	$k_{photo} \times 10^3$	R^2_{photo}
PP@TiO_2	2.54	0.9963	7.70	0.9960
PP@0.060rGO-TiO_2	3.93	0.9965	10.10	0.9889
PP@0.125rGO-TiO_2	3.78	0.9978	11.20	0.9971
PP@0.150rGO-TiO_2	3.54	0.9979	8.89	0.9994
PP@0.188rGO-TiO_2	3.86	0.9940	7.73	0.9939
PP@0.250rGO-TiO_2	3.66	0.9964	8.41	0.9937

*M. Zannotti et al. Catalysts **2018**, 8, 598*

ADSORBENT MATERIAL FOR ENVIRONMENTAL APPLICATION

Chemistry Interdisciplinary Project

CELLULOSE AEROGEL

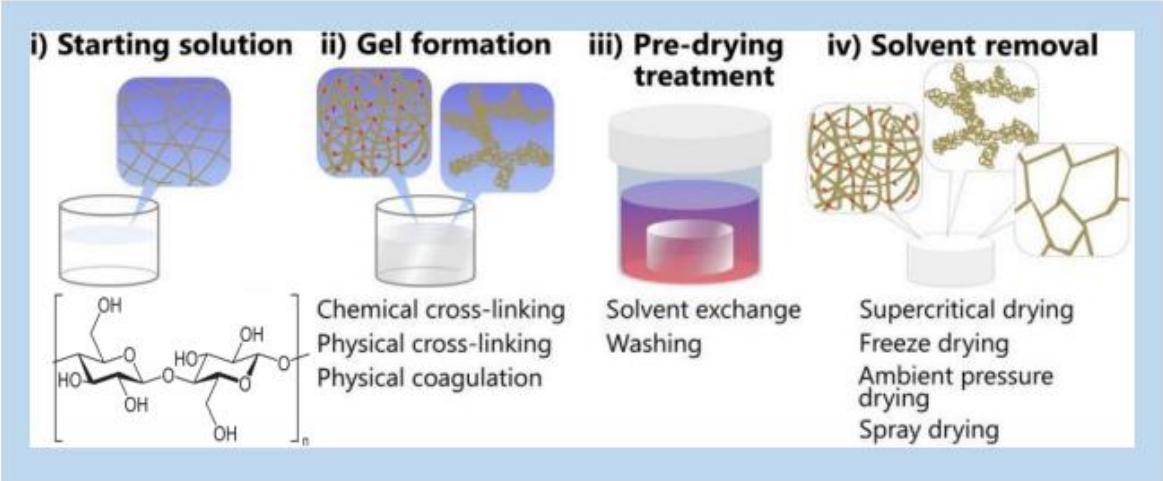

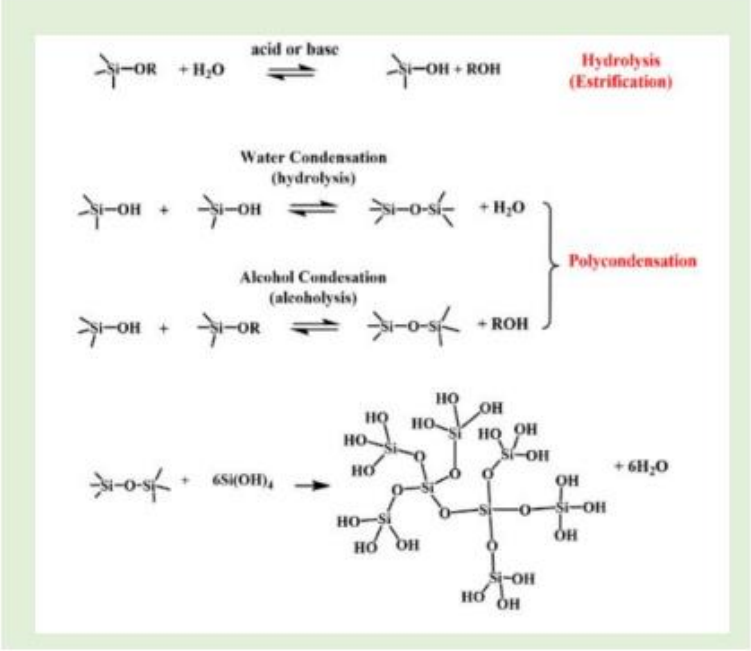

SILICA-BASED XEROGEL

ADSORBENT MATERIAL FOR ENVIRONMENTAL APPLICATION

Chemistry Interdisciplinary Project

CELLULOSE AEROGEL

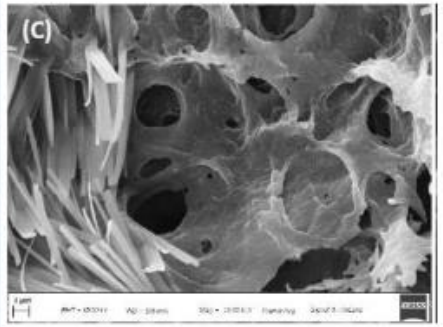

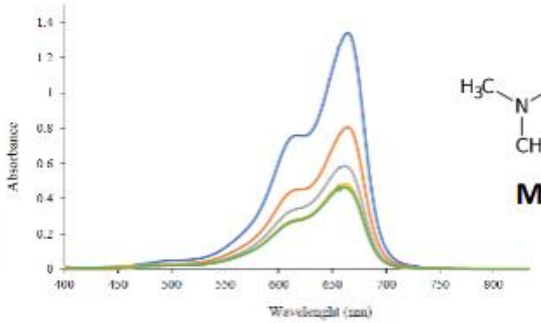

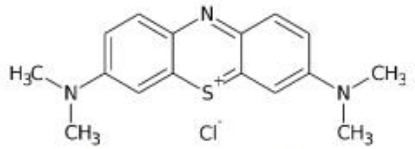

Methylene Blue (MB)

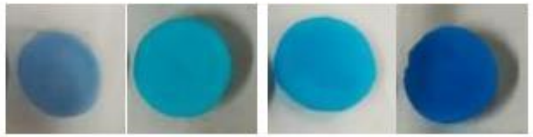

Increasing concentration of MB

CELLULOSE AEROGEL & graphene

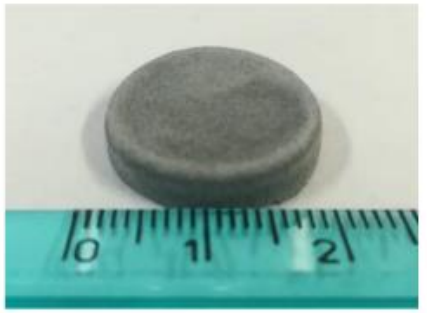

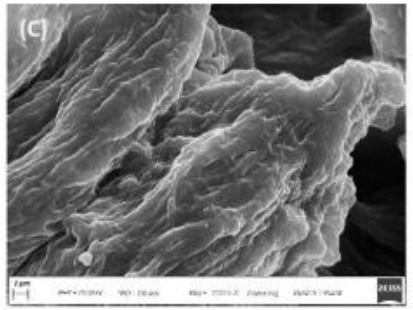

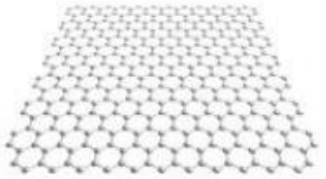

Graphene

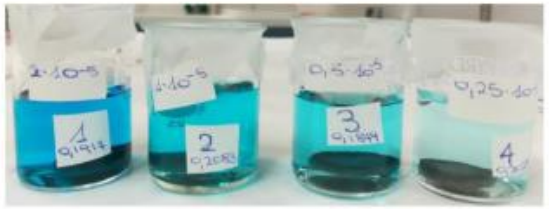

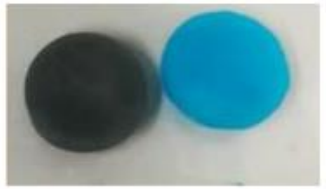

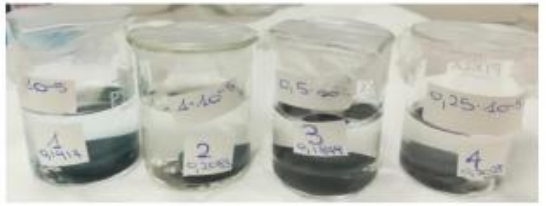

ADSORBENT MATERIAL FOR ENVIRONMENTAL APPLICATION

Università di Camerino

Chemistry Interdisciplinary Project

SILICA-BASED XEROGEL

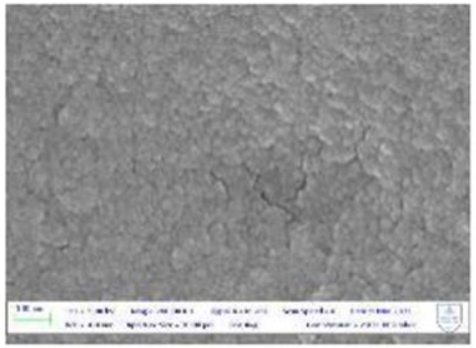

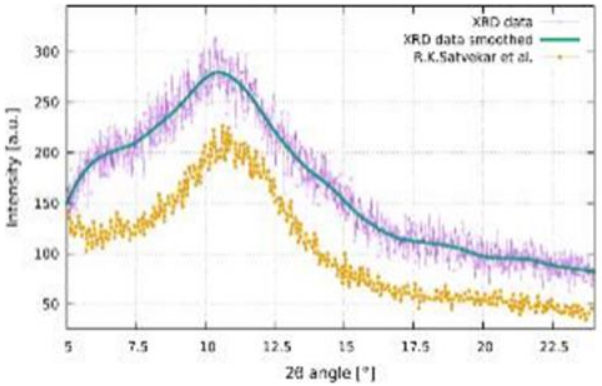

Increasing concentration of Cr(VI)

$S_{surf}—OH + H_3O^+ \rightleftharpoons S_{surf}—OH_2^+ + H_2O \xrightarrow{\text{Cr(VI) solution}} S_{surf}—OH_2^+/HCrO_4^-$

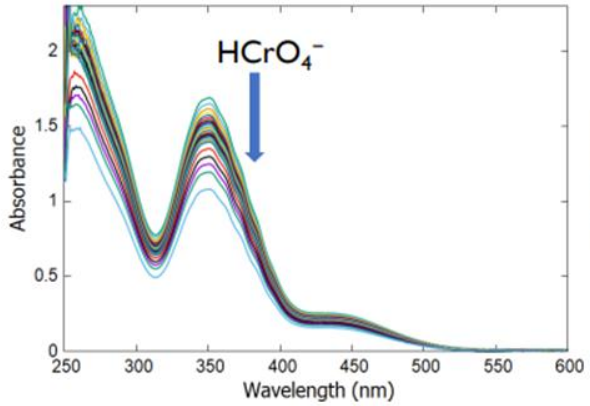

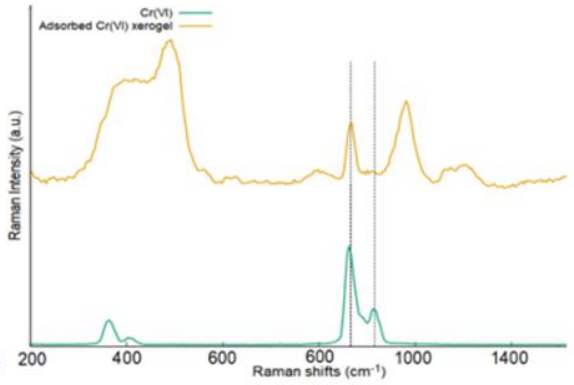

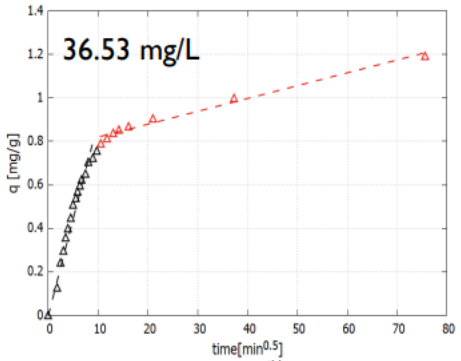

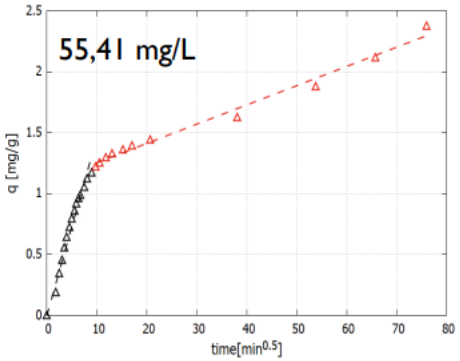

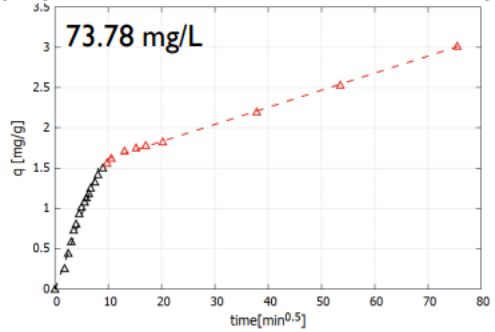

Freundlich Isotherm Model	
$1/n$	1.0742
lnK_F	3.5333
K_F	0.0292
R^2	0.9812

Cr(VI) (mg/L)	Intraparticle Diffusion $q_t = k_{id}t^{1/2} + C$					
	Phase 1			Phase 2		
	kd_1 (mg/g min$^{0.5}$)	Duration (min)	R^2	kd_2 (mg/g min$^{0.5}$)	Duration (min)	R^2
36.53	0.0891	90	0.9712	0.0069	—	0.9879
55.41	0.1462	80	0.9734	0.0158	—	0.987
73.78	0.1745	80	0.9762	0.0212	—	0.9978

Freundlich Isotherm
lnCe vs lnQe

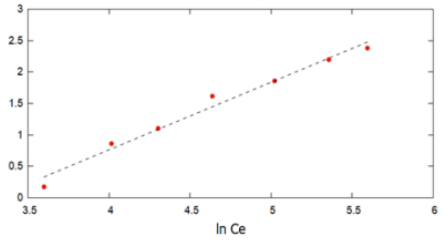

Langmuir Isotherm
Ce/Qe vs Ce

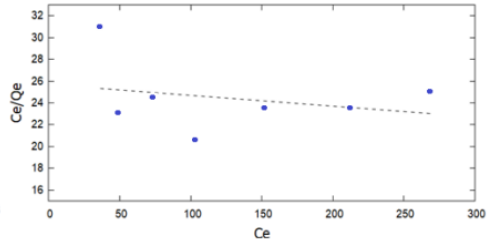

CARBON CAPTURES: NATURAL GAS HYDRATES

Ministero dell'Istruzione, dell'Università e della Ricerca

MIUR

PRIN 2017
Methane recovery and carbon dioxide disposal in natural gas hydrate reservoirs

Chemistry Interdisciplinary Project